Vilnius University
Faculty of Physics
Department of General Physics and Spectroscopy

Dovilė Lengvinaitė

# MOLECULAR DYNAMICS SIMULATIONS OF 1-DECYL-3-METHYL-IMIDAZOLIUM CHLORIDE IONIC LIQUID AND ITS MIXTURES WITH WATER

Master thesis

Environmental and chemical physics

| | |
|---|---|
| Student | Dovilė Lengvinaitė |
| Supervisors | Dr. Kęstutis Aidas |
| | Prof. Francesca Mocci |
| Reviewer | Lec. Mantas Šimėnas |
| Head of the department | Prof. Dr. (HP) V. Šablinskas |

Vilnius 2016

Vilniaus universitetas
Fizikos fakultetas
Bendrosios fizikos ir spektroskopijos katedra

Dovilė Lengvinaitė

# JONINIO SKYSČIO 1-DECIL-3-METIL-IMIDAZOLO CHLORIDO IR JO MIŠINIŲ SU VANDENIU MOLEKULINĖS DINAMIKOS SIMULIACIJOS

Magistratūros studijų baigiamasis darbas

Aplinkos ir cheminė fizika

| | |
|---|---|
| Studentas | Dovilė Lengvinaitė |
| Darbo vadovai | Dr. Kęstutis Aidas |
| | Prof. Francesca Mocci |
| Recenzentas | Lekt. Mantas Šimėnas |
| Katedros vedėjas | Prof. Dr. (HP) V. Šablinskas |

Vilnius 2016

# Content

# Introduction

Ionic liquids (ILs) are salts that have a melting point below 100 ºC. Many ILs remain liquid at or near room temperature and are called room-temperature ionic liquids (RTILs).[1] Ionic liquids are typically composed of organic cations and mostly inorganic anions, and they have attracted considerable attention as they have many potential applications in separations, organic synthesis, catalysis and electrochemical devices.[2-7] These liquids are considered as "green" and environmentally friendly solvents because they are nonvolatile, thermally stable and recyclable. Because ILs can be formed by combining a large variety of cations and anions, they possess a great versatility of their chemical and physical properties such as negligible vapor pressure, viscosity, high thermal stability and electrical conductivity. Therefore, ILs can be tailored and tuned for specific tasks, so that they are referred "designer" solvents.[8]

Due to their unique and attractive properties, ionic liquids are intensively investigated using different theoretical and experimental techniques. The physical properties for RTILs over large ranges of temperature and pressure, including melting points, densities, viscosities, solubilities, liquid-liquid phase equilibrium, heat capacities, etc, have been reported.[9] Structure and dynamics of these liquids have been studied by different techniques, such as neutron diffraction,[10-11] NMR spectroscopy,[12-15] IR and Raman spectroscopy,[16-17] as well as classical molecular dynamics (MD) simulations,[18-24] and quantum-chemical calculations.[14, 25-29] It is obvious that understanding of these novel solvents has considerably improved. However, despite an enormous number of works on ILs applying variety of experimental techniques and theoretical methods, the relationships between properties and structure of ILs are still poorly understood.

In the last several years, RTILs have become an interesting class of solvents for different chemical applications and required a better understanding of their physical and chemical properties. The family of ILs based on imidazolium cations has been intensively investigated due to their atrractive physical and chemical properties.[30-31] A number of experimental and theoretical studies of imidazolium-based ILs have focused on understanding the interactions between different types of ILs and water solvent. Understanding of these interactions is of great importance because ILs can absorb a large amount of water from the atmosphere.[32-36] This is relevant due to the fact that even low levels of water in ILs can dramatically change their physical and chemical properties such as viscosity, density, conductivity and solvating ability. It has been reported for imidazolium-based ILs that hydrophobicity increases with the length of the cations' alkyl tail and the size of anions.[37] Cammarata et al.[38] found, experimentally, that in both hydrophilic and hydrophobic 1-alkyl-3-methylimidazolium ILs, water molecules tend to be isolated from each other or exist in small independent clusters in mixtures with less ions than water molecules. When the molar proportion of water molecules reaches 75%, a continuous network of water is found as a predominated water

structure which changes the properties of the mixture dramatically.[39]

Additionally, various computational methods, such as molecular dynamics simulations,[40-44] COSMO-RS,[45] and quantum mechanics calculations[46] have been used to examine the interaction of different types of solutes in IL−water mixtures. Molecular dynamics simulations of the structure and dynamic properties of IL−water mixtures have been performed on 1,3-dimethylimidazolium chloride ([MMim][Cl]) and 1,3-dimethylimidazolium hexafluorophosphate ([MMim][$PF_6$]) mixed with water.[37] Jiang et al.[48] studied the effect of water content on the nanostructural organization in 1-octyl-3-methylimidazolium ([OMim][$NO_3$])−water mixtures. Fang and Voth[49] have analyzed the influence of both alkyl chain length and anion on the structure and dynamics of three ILs (1-butyl-3-methylimidazolium hexafluorophosphate ([BMim][$PF_6$]), 1-octyl-3-methylimidazolium tetrafluoroborate ([OMim][$BF_4$]) and 1-octyl-3-methylimidazolium chloride ([OMim][Cl])) mixed in water. Recently, Hall and co-workers[50] have experimentally studied macroscopic and microscopic properties of 1-ethyl-3-methylimidazolium acetate ([EMim][Ac])−water mixtures at different composition range from pure IL to pure water.

The aim of this work is to study the structural and dynamical properties of the ionic liquid 1-decyl-3-methyl-imidazolium chloride ([DMim][Cl]) and investigate how they are affected by the presence of water molecules.

In order to meet formulated objective, following tasks were raised:

- ✓ Perform short MD simulations of the pure [DMim][Cl] ionic liquid and analyze the effect of parameters such as the cutoff radius of Van der Waals interactions, and integration time step on the results of the simulations.
- ✓ Perform MD simulations of the pure [DMim][Cl] ionic liquid and [DMim][Cl]/water systems with various concentrations of water using the best settings in term of accuracy and computational time.
- ✓ Evaluate the structural and dynamical properties of the [DMim][Cl] ionic liquid and study how they are affected by the presence of water molecules.

# 1. Theoretical outline

## 1. 1. Molecular dynamics simulations

Molecular dynamics (MD) simulations is a technique for computing the structural, thermodynamic and transport properties of a many-body system. Molecular dynamics simulations of atomic or molecular systems aim to provide information about the properties of a macroscopic sample. The atoms and molecules are allowed to interact for a fixed period of time, giving a view of the dynamical evolution of the system. The principle of the molecular dynamics simulation is the solution of the classical Newton's equations of motion for many-body system. MD simulations are mostly used in chemical physics, material sciences and biochemical sciences.

There are two main families of MD methods, which can be distinguished according to the model chosen to represent a physical system. In the 'classical' mechanics approach to MD simulations molecules are treated as classical objects, resembling the 'ball and stick' model. Atoms are represented by point particle and bonds are approximated by elastic springs. The laws of classical mechanics define the dynamics of the system. The 'quantum' or 'first-principles' MD simulations, which were introduce in the 1980s in the seminal work of Car and Parrinello, take explicitly into account the quantum nature of the chemical bond. The electron density function for the valence electrons that determine bonding in the system is computed using quantum chemical equations, while the dynamics of atoms is described classically. MD simulation based on quantum mechanics is more accurate than classical and is widely used to study small molecular structures. However, these simulations allow to study molecular dynamics on relatively short time and require very large computational resources. This is main reason why the classical molecular dynamics simulations are often used to perform simulations of large systems.[51]

Molecular dynamics simulations run in accordance with clearly defined algorithm (see Figure 1.1). First of all, each molecular dynamics simulation starts with the determination of the initial conditions, such as system temperature, volume, number of particles, the simulation duration, molecular structural parameters, etc.[52] MD simulations are usually performed on a number of molecules on the scale of $10^1 \leq N \leq 10^6$. The size of the system is limited by the available storage on the host computer. To start the simulation, it is necessary to assign initial positions and velocities to all particles in the system. The particle positions should be chosen compatible with the structure that one is aiming to simulate. The next step is the calculation of the forces acting on every particle using a defined force field in classical MD simulation or by solving appropriate Schrödinger equation in quantum mechanics. The essential idea is that the integration is broken down into many small stages, each separated in time by a fixed time period, called integration time step $\Delta t$. The total force on each particle in the configuration at time *t* is calculated as the vector sum of potential

forces each neighboring particle is exerting upon the particle at hand. Once the forces have been computed, the accelerations of the particles can now be determined, which are then combined with the positions and velocities at a time *t* to calculate the positions and velocities at a time $t + \Delta t$. The force is assumed to be constant during the time step. The forces on the particles in their new positions are then determined, leading to new positions and velocities at time $t + 2\Delta t$, and so on. Calculations are repeated until the time evolution of a system reaches the desired length of time. In the last step, the final configurations of particles are extracted and the simulation is completed.

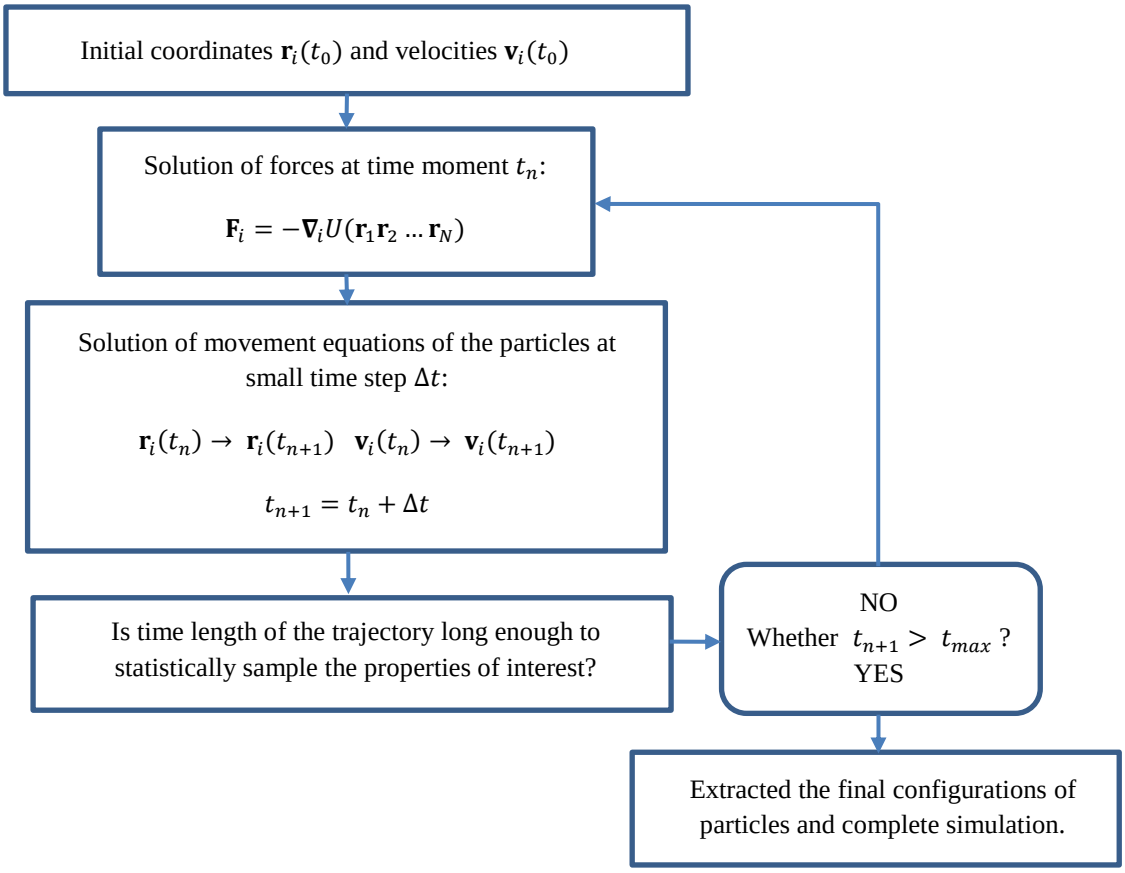


**Figure 1.1** The algorithm of the MD simulation

### 1.1.1 Periodic boundary conditions

The simplest method of constructing a liquid structure is to place molecules at random inside the simulation box. However, a realistic model of a solution requires at least several hundred solvent molecules. To prevent the outer solvent molecules from boiling off into space and to minimize surface effects, periodic boundary conditions are normally employed. This cubic box is replicated throughout space to form infinite lattice. In the course of the simulation, as a molecule moves in the original box, its periodic image in each of the neighbouring boxes moves in exactly the same way. Thus, as a molecule leaves the central box, one of its images will enter through the opposite face. There are no walls at the boundary of the central box and no surface molecules.[53]

This box simply forms a convenient axis system for measuring the coordinates of the N molecules. A two-dimentional version of such a periodic system is shown in Figure 1.2. Otherwise, there is a problem if all intermolecular interactions are included in the system, then the total number of the calculations of interactions is infinite. In practice, we are often dealing with short-range interaction because the strength of interaction falls as 1/r. Due to permissible to truncate all intermolecular interactions beyond a certain cutoff distance $r_c$. The error that results when interactions with particles are ignore at larger distances can be made arbitrarily small by choosing $r_c$ sufficiently large. The cutoff distance must be no greater than *L/2* (half the diameter of the periodic box) for consistency with the minimum image convention.[51]

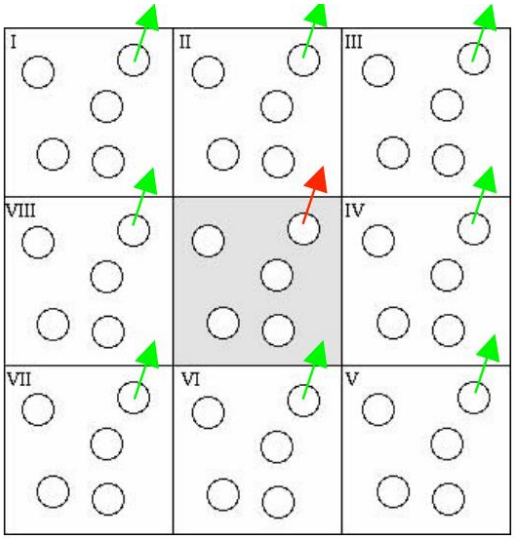


**Figure 1.2** Scheme of the two-dimentional periodic boundary system

### 1.1.2 Ensembles

MD simulation generates information at the microscopic level (atomic and molecular positions, velocities, etc.) and the conversion of this very detailed information into macroscopic terms (pressure, internal energy, etc.) is the province of statistical mechanics. The thermodynamic state of a system is usually defined by a small set of parameters such as the number of particles *N*, the temperature *T*, the pressure *P* and volume, *V*. Other thermodynamic properties (chemical potential $\mu$, heat capacity $C_V$ and etc.) may be derived through on knowledge of the equations of state and the fundamental equations of thermodynamics.

The molecular dynamics technique is a scheme for studying the natural time evolution of a classical system of *N* particles in volume *V* at temperature *T*. In such simulations, the total energy *E* is a constant of motion. MD simulations can be carried out at constant number of particle *N*, the volume *V* and energy *E* and it is called microcanonical *NVE* ensemble. However, the MD simulations are usually performed in the *NVT* or *NPT* ensembles. NVT is the canonical ensemble, where the number of particles, volume and temperature are conserved. The temperature of the

system is directly related to the kinetic energy therefore the temperature can be controlled by changing the particle velocities. Mostly used techniques to control temperature are Berendsen, Andersen, Nose-Hoover thermostats.[54] NPT is isothermal-isobaric ensemble, where the number of particles, pressure and temperature are conserved. The temperature and pressure of the system are controlled by changing the volume through barostat and thermostat. It should be noted that the dimensions of box must change uniformly.[55]

### 1.1.3 Force fields

The accuracy of MD simulations to predict parameters of various systems depends on the force field model. A force field is a mathematical expression describing the dependence of the energy of a system on the coordinates of its particles. The parameters are typically obtained either from ab initio or semi-empirical quantum mechanical calculations or by fitting to experimental data for example neutron, X-ray and electron diffraction, NMR, infrared, Raman and neutron spectroscopy.[55] Force fields can be divided into two groups: all atom and united atom. The first type of force field attributes parameters for each atom contained in the system, including hydrogens. The second type of force field attributes parameters for each atom contained in the system, with the exception of hydrogens, which belongs to the methyl or methylene groups, such groups are assigned to the parameters as a single atom.[52] The first force fields appeared in the 1960's, with the development of the molecular mechanics (MM) method, and their primary goal was to predict molecular structures, vibrational spectra and enthalpies of isolated molecules.[56] Currently, the most widely used force fields, such as CHARMM[57], AMBER [58], GROMOS[59], OPLS[60] and COMPASS,[61] are adapted for large and complex systems. The force fields are divided into non-polarizable and polarizable. During the 1990s the first general polarizable force fields appeared. Polarizable force field increases the accuracy of the simulation and provides more accurate information about the microscopic and thermodynamic properties.

The intermolecular interactions between atoms are described by using a potential function of force field as accurate equations of force in MD simulation. There are many force fields available in the literature, having different degrees of complexity, and oriented to treat different kinds of systems. However, a typical expression for force field may look like this:

$$U = \sum_{bonds} \frac{1}{2} k_b (r - r_0)^2 + \sum_{angles} \frac{1}{2} k_a (\theta - \theta_0)^2 + \sum_{dihedrals} \frac{V_n}{2} [1 + cos(n\phi - \delta)] + \sum_{LJ} 4\epsilon_{ij} \left( \frac{\sigma_{ij}^{12}}{r_{ij}^{12}} - \frac{\sigma_{ij}^{6}}{r_{ij}^{6}} \right) + \sum_{elec} \frac{q_i q_j}{r_{ij}}. \quad (1.1)$$

where the first three terms refer to intramolecular or local contributions to the total energy (bond stretching, angle bending and torsions) and the last two terms serve to describe the non-bonded

interactions, including Van der Waals and the Coulombic interactions. Electrostatic and Van der Waals interactions are calculated between atoms in different molecules or for the atoms in the same molecule separated by more than three bonds. Van der Waals interactions are expressed by the Lennard-Jones (LJ) potential. The LJ potential is a mathematical model which describes interactions between neutral atoms or pairs of molecules. A typical expression for LJ potential is written as:

$$E_{LJ_{ij}} = 4\epsilon_{ij}\left[\left(\frac{\sigma_{ij}^{12}}{r_{ij}^{12}}\right) - \left(\frac{\sigma_{ij}^{6}}{r_{ij}^{6}}\right)\right], \tag{1.2}$$

where $\epsilon_{ij}$ is the traditional well-depth, $\sigma_{ij}$ is the finite distance at which the inter-particle potential is equal to zero, $r_{ij}$ is distance between particles $i$ and $j$. The first term of the expression of LJ potential describes short-range repulsion forces, which occurs due to overlapping electron clouds, the second term describes long-range attractive forces, which is due to the dispersion (see Figure 1.3).

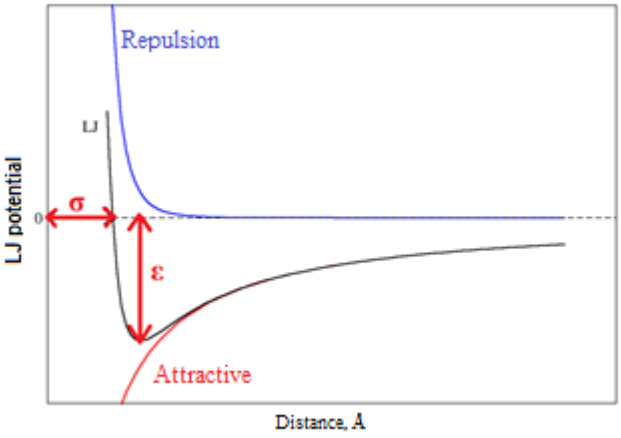


**Figure 1.3** Lennard-Jones potentials

The LJ parameters for unlike atoms are obtained from the Lorentz-Berthelot (LB) combining rule:

$$\epsilon_{ij} = \sqrt{\epsilon_i \epsilon_j}, \tag{1.3}$$

$$\sigma_{ij} = \frac{(\sigma_i + \sigma_j)}{2}. \tag{1.4}$$

Lennard-Jones potential is a good method to describe an interactions and because of its simplicity widely used in molecular simulations.

### 1.1.4 Integration of the equations of motion

The calculation of the force acting on every particle is the most time-consuming part of

almost all molecular dynamics simulations. Here, it is important to evaluate the contribution to the force on particle *i* due to all its neighbors. If we consider only the interaction between a particle and the nearest image of another particle, this implies that, for a system of N particles, we must evaluate *N x (N-1)/2* pair distances. This implies that, the time needed for the evaluation of the forces scales as $N^2$. There exist efficient techniques to speed up the evaluation of both short-range and long-range forces in such a way that the computing time scales as *N*, rather than $N^2$.

Own, the forces between the particles have been computed, integration of Newton's equations of motion follows. The Verlet algorithm is probably the most widely used method of integrating the equations of motion in a molecular dynamics simulation. This algorithm assumes that the positions and dynamic properties can be approximated as Taylor expansion of the coordinate of a particle, around time *t*,

$$r(t+\Delta t) = r(t) + v(t)\Delta t + \frac{f(t)}{2m}\Delta t^2 + \frac{\Delta t^3}{3!}\dddot{r} + \vartheta(\Delta t^4), \tag{1.5}$$

similarly,

$$r(t-\Delta t) = r(t) - v(t)\Delta t + \frac{f(t)}{2m}\Delta t^2 - \frac{\Delta t^3}{3!}\dddot{r} + \vartheta(\Delta t^4). \tag{1.6}$$

Adding these two equations gives

$$r(t+\Delta t) + r(t-\Delta t) = 2r(t) + \frac{f(t)}{2m}\Delta t^2 + \vartheta(\Delta t^4) \tag{1.7}$$

or

$$r(t+\Delta t) \approx 2r(t) - r(t-\Delta t) + \frac{f(t)}{2m}\Delta t^2. \tag{1.8}$$

The estimation of the new position contains an error that is of order $\Delta t^4$, where $\Delta t$ is the time step in molecular dynamics scheme. Note that Verlet algorithm does not use the velocity to compute the new position of particle. However, the velocity is derived from knowledge of the positions of the molecules, using

$$r(t+\Delta t) - r(t-\Delta t) = 2v(t)\Delta t + \vartheta(\Delta t^3) \tag{1.9}$$

or

$$v(t) = \frac{r(t+\Delta t) - r(t-\Delta t)}{2\Delta t} + \vartheta(\Delta t^2). \tag{1.10}$$

This expression for the velocity is only accurate to order $\Delta t^2$.

Several other algorithms are equivalent to the Verlet scheme. The most popular is the so-called Leap Frog algorithm. This algorithm evaluates the velocities at half-integer time steps and uses these velocities to compute the new positions. To derive the Leap Frog algorithm from the Verlet scheme is necessary to start by defining the velocities at half-integer time steps as follows:

$$v(t - \Delta t/2) \equiv \frac{r(t)-r(t-\Delta t)}{\Delta t} \quad (1.11)$$

and

$$v(t + \Delta t/2) \equiv \frac{r(t+\Delta t)-r(t)}{\Delta t}. \quad (1.12)$$

From the latter equations, an expression for the new positions is obtained based on the previous positions and velocities:

$$r(t + \Delta t) = r(t) + \Delta t v(t + \Delta t/2). \quad (1.13)$$

The following expression is used update to the velocities:

$$v(t + \Delta t/2) = v(t - \Delta t/2) + \Delta t \frac{f(t)}{m}. \quad (1.14)$$

As the Leap Frog algorithm is derived from the Verlet algorithm, it gives rise to identical trajectories. Note, however, that the velocities are not defined at the same time as positions. As a consequence, kinetic and potential energy are also not defined at the same time, and hence we cannot directly compute the total energy in the Leap Frog scheme.[52]

### 1.1.5 Radial distribution functions and the coordination number

Radial distribution functions (RDFs) are a useful way to describe the structure of a system, particularly of liquids. It can be defined as the ratio between the local density on a sphere shell of thickness $dr$ at a distance $r$ from the chosen atom and the average density (see Figure 1.4).[55] The radial distribution function is expressed by a simple equation:

$$g(r) = \frac{dN}{4\pi r^2 \rho dr}, \quad (1.15)$$

here $\rho = \frac{N}{V}$ – density of system, where $N$ is number of particles, $dN$- number of particles which belongs to layer of thickness $dr$, $V$- volume, $r$ – distance between particles, $4\pi$ – spatial angle.

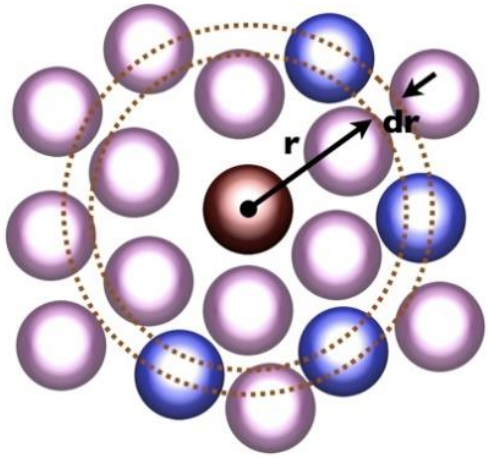


**Figure 1.4** The visualization of calculation of *g(r).*

The radial distribution function, *g(r)*, gives the probability of finding an atom or molecule a distance *r* from another atom or molecule, relative to the probability expected for a completely random distribution at the same density. The radial distribution function will typically have a structure as shown in Figure 1.5 for a simulation of liquid. This type of graph provides a lot of structural information about the structural properties such as distribution of solvation layers and determines the probability of finding the particle B around particle A.

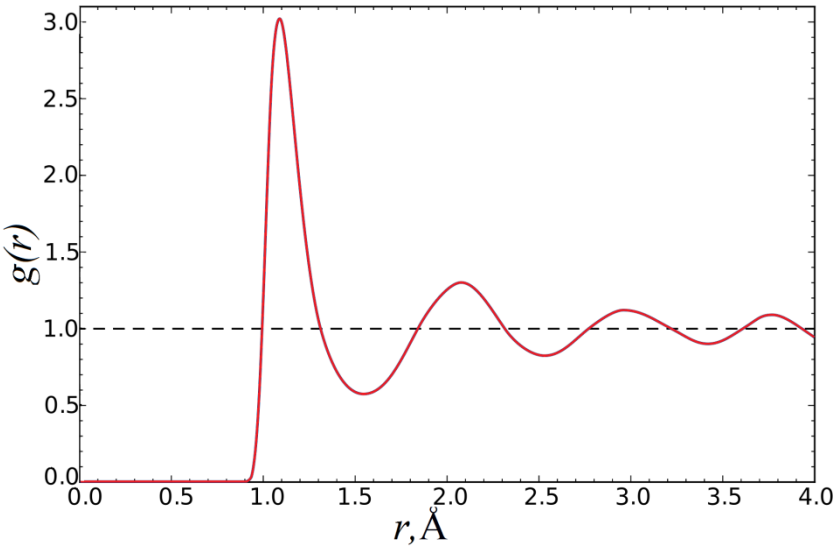


**Figure 1.5** The radial distribution function of a liquid

Integration of the RDFs to the first minimum gives a coordination number which is an average number of neighbors in the first coordination sphere.[62] It becomes hydration number if the RDF is calculated between a solute (an ion for example) and the solvating water molecules. Hydration number can be determined in NMR spectroscopy and compared directly with simulated results. Many internal structural changes can be studied by calculating RDFs or other types of population distributions and compared with NMR measurements. The coordination number is calculated by integrating the radial distribution function:

$$n_c = 4\pi\rho \int_{r_1}^{r_2} r^2 g(r) dr, \tag{1.16}$$

here $4\pi$ – spatial angle, $\rho$ – density of system, $r$ – distance between particles, $g(r)$ – radial distribution function.

### 1.1.6 Spatial distribution functions

Spatial distribution functions (SDFs) can be considered as the extension of RDFs to three dimensions thereby giving orientational information concerning the interaction, which cannot

be obtained from the RDF. Fixing a local coordinate system in the reference molecule, or on a portion of it, spatial pairwise correlations are calculated within the local frame as vectors. Apart from this difference, SDF is defined in the same way as RDF,

$$S_{AB}(\vec{r}) = \frac{\rho_B \langle \vec{r} | \vec{r}_A = 0 \rangle}{\rho_B}. \tag{1.17}$$

In the Cartesian space it can be calculated as:

$$S_{AB}(i,j,k) = \langle \frac{1}{N_A} \sum_{n_A=1}^{N_A} \sum_{n_B=1}^{N_B} I_{i,j,k} \left[ R_{n_A}^A \left( \vec{r}_{n_B}^B - \vec{r}_{n_B}^A \right) \right] \rangle, \tag{1.18}$$

where $R_{n_A}^A$ is a rotational transformation matrix from laboratory frame to molecular frame fixed on molecule A and $I_{ijk}$ is used to collect the three-dimentional spatial populations of site B.

SDFs will most likely turn out to be most convenient tools in MD simulations to study the liquid structure and molecular organization in ionic liquid systems (see Figure 1.6). Because of the strong interactions between the unlike ions, the life time of the coordinated structures becomes longer, making it easier to reach convergence in calculating the SDFs.[62]

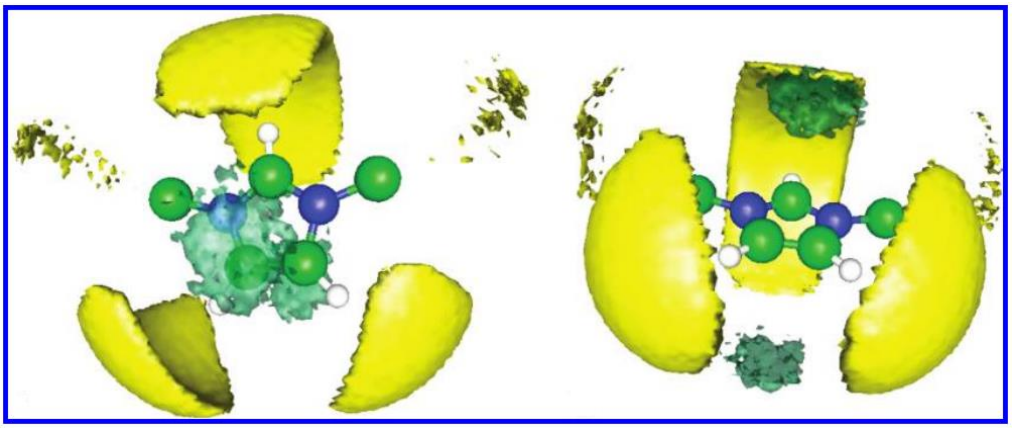

**Figure 1.6** The typical SDFs of chloride anion (yellow) and carbon (green) on cations around cations in ionic liquid [C1mim][Cl].[63]

### 1.1.7 Diffusion coefficient

Diffusion is caused by the random motion of the particles in the fluid. The macroscopic law that describes diffusion is known as Fick's law, which states that the flux $\boldsymbol{j}$ of the diffusing species is proportional to the negative gradient in the concentration of that species:

$$\boldsymbol{j} = -D\boldsymbol{\nabla} c, \tag{1.19}$$

where *D*, the constant of proportionality, is referred to as the diffusion coefficient. Diffusion of a labeled species among otherwise identical solvent molecules is called self-diffusion. In order to find the expression of diffusion coefficient it is necessary to find the function, describing the time

evolution of the concentration of substance.

$$\frac{\partial c(r,t)}{\partial t} + \boldsymbol{\nabla} \cdot \boldsymbol{j}(r,t) = 0. \tag{1.20}$$

Combining equation (1.20) with equation (1.19), we obtain

$$\frac{\partial c(r,t)}{\partial t} - D\nabla^2 \cdot c(r,t) = 0. \tag{1.21}$$

In fact, we do not need to find $c(r,t)$ itself, it is enough to calculate the mean-square distance of the particles as a dependency of time:

$$\langle r^2(t) \rangle \equiv \int d\mathbf{r}\, c(r,t) r^2, \tag{1.22}$$

We can directly obtain an equation for the time evolution of $\langle r^2(t) \rangle$ by multiplying equation (1.21) by $r^2$ and integrating over all space. This yield

$$\frac{\partial}{\partial t} \int d\mathbf{r}\, r^2 c(r,t) = D \int d\mathbf{r}\, r^2 \nabla^2 c(r,t). \tag{1.23}$$

The left-hand side of this equation is simply equal to

$$\frac{\partial \langle r^2(t) \rangle}{\partial t}. \tag{1.24}$$

Applying partial integration to the right-hand side, we obtain

$$\begin{aligned} \frac{\partial \langle r^2(t) \rangle}{\partial t} &= D \int d\mathbf{r}\, r^2 \nabla^2 c(r,t) = D \int d\mathbf{r}\, \boldsymbol{\nabla} \cdot \left( r^2 \boldsymbol{\nabla} c(r,t) \right) - D \int d\mathbf{r}\, \boldsymbol{\nabla} r^2 \cdot \boldsymbol{\nabla} c(r,t) \\ &= D \int d\mathbf{S} \left( r^2 \boldsymbol{\nabla} c(r,t) \right) - 2D \int d\mathbf{r}\, \mathbf{r} \cdot \boldsymbol{\nabla} c(r,t) \\ &= 0 - 2D \int d\mathbf{r} \left( \boldsymbol{\nabla} \cdot \mathbf{r} c(r,t) \right) + 2D \int d\mathbf{r}\, (\boldsymbol{\nabla} \cdot \mathbf{r}) c(r,t) \\ &= 0 - 2dD \int d\mathbf{r}\, c(r,t) = 2dD, \end{aligned} \tag{1.25}$$

*d* denotes the dimensionality of the system.

Equation (1.25) relates the diffusion coefficient *D* to the width of the concentration profile. This relation was first derived by Einstein. It should be realized that, whereas *D* is a macroscopic transport coefficient, $\langle r^2(t) \rangle$ has a microscopic interpretation: it is the mean-squared distance over which the labeled molecules have moved in a time interval *t*. This immediately suggests how to measure *D* in a computer simulation. For every particle *i*, we measure the distance traveled in time t, $\Delta \mathbf{r}_i(t)$, and we plot the mean square of these displacement as a function of the time t:

$$\langle \Delta r(t)^2 \rangle = \frac{1}{N} \sum_{i=1}^{N} \Delta \mathbf{r}_i\,(t)^2 = \frac{1}{N} \sum_{i=1}^{N} \left( \Delta \mathbf{r}_i(t) - \mathbf{r}_i(0) \right)^2. \tag{1.26}$$

On the other hand, the displacement that we are interested in is simply the time integral of the

velocity of the tagged particle:

$$\Delta\mathbf{r}(t) = \int_0^t dt'\,\mathbf{v}(t'). \tag{1.27}$$

In fact, there is a relation that expresses the diffusion coefficient directly in terms of the particle velocities. We start with the relation:

$$2D = \lim_{t\to\infty} \frac{\partial\langle x^2(t)\rangle}{\partial t}, \tag{1.28}$$

where for convenience, we consider only one Cartesian component of the mean-squared displacement.

# 2. Details of the simulation

All MD simulations were performed using AMBER package.[63] Figure 2.1 shows the molecular structure and atom-numbering scheme for the [DMim][Cl] of ionic liquid simulated in this work. We prepared one small pure IL system and three different systems, with the mole fraction of water varying from 0 (pure IL) to 0.12 and 0.46 (dilution of the IL), respectively. The initial configurations were built using PACKMOL program package.[64]

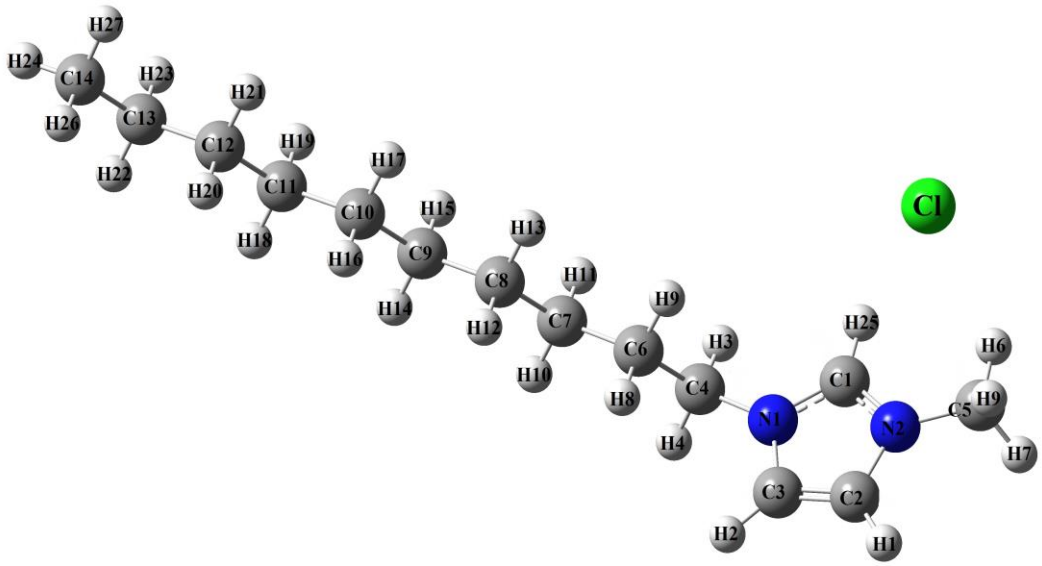


**Figure 2.1** Labeled atoms of [DMim][Cl] ionic pair

The force field is expressed as the functional form in AMBER:

$$E = \sum_{bonds} K_r(r - r_0)^2 + \sum_{angles} K_\theta(\theta - \theta_0)^2 + \sum_{dihedrals} \frac{K_\phi}{2}[1 + cos(n\phi - \gamma)] + \sum_{i<j}\left[\frac{A_{ij}}{r_{ij}^{12}} - \frac{B_{ij}}{r_{ij}^{6}} + \frac{q_i q_j}{r_{ij}}\right]. \quad (2.1)$$

The first three terms represent the bonded interactions, i.e., vibrations of bonds, angles and torsional motion. The non-bonded interactions are described in the last term, including van der Waals (VDW, in the Lennard-Jones (LJ) 6-12 form) and Coulombic interactions of atom-centered point charges. Electrostatic and VDW interactions are calculated between the atoms in different molecules or for the atoms in the same molecule separated by more than three bonds. The non-bonded interactions separated by exactly three bonds (1-4 interactions) are reduced by a scale factor, which is optimized as 1/2 for VDW and 1/1.2 for electrostatic interactions.

Force field parameters for the [DMim] cation as well as the chloride anion were taken

from the work of Liu et al.[66] Water was simulated using the TIP4P water model. For all systems C−H and O-H bonds were held rigid using the SHAKE algorithm.[67] For all systems, a cutoff distance (9 Å) was used for non-bonded interactions. The initial simulation boxes were cubes with sides of length 50 Å and 75 Å (respectively for 125 and 375 ionic pairs), typically much larger than its equilibrium size. It is well-known that the dynamics of ILs is very slow and the simulation results probably depend on the initial state. Thus, to fix the system density, systems were equilibrated by running several simulations following steps in Figure 2.2. The simulations were performed in the isothermal−isobaric (NPT) ensemble before beginning production runs at 350 K with 2 fs time steps. For NPT simulations, a Berendsen thermostat was used. For each simulation, the positions of the atoms were dumped into trajectory files every 5 ps.

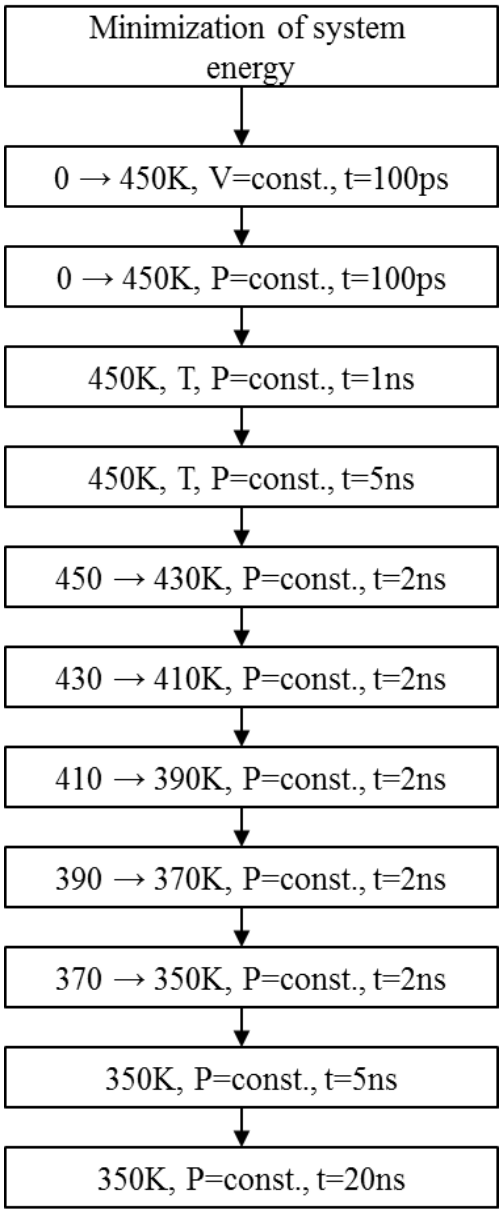


**Figure 2.2** Steps to reach equilibration of the systems

The single-ion trajectories were used to estimate the diffusivity of the IL as a function of water concentration. Diffusion coefficients have been determined by fitting the mean square displacement (MSD) data using the Einstein relation:

$$D = \frac{1}{6}\frac{\partial\langle\Delta r^2(t)\rangle}{\partial t},\ \langle\Delta r^2(t)\rangle = \langle\left(\vec{r}(t_0+t) - \vec{r}(t_0)\right)^2\rangle, \quad (2.2)$$

where the angle brackets denote ensemble averages.

# 3. Results and discussion

### 3.1 Time step estimation

It is well-know that one of the often issue is to select the appropriate integration time step for a molecular dynamics simulations; too small and the trajectory will cover only a limited portion of the phase space; too large and instabilities may arise in the integration algorithm due to high energy overlaps between atoms. Thus, to estimate influence of integration time step for structural and dynamical properties of pure ionic liquid, we performed simulation of pure ionic liquid using different integration time steps. The figure 3.1 shows the comparison of density between different integration time steps (respectively 2 fs and 0.2 fs) which were calculated during 200 ns and 80 ns isothermal-isobaric MD simulations of pure [DMim][Cl] ionic liquid at 350 K. It should be noted, that MD simulation was performed using SHAKE[67] algorithm at integration time step 2 fs and without SHAKE algorithm at integration time step 0.2 fs. The results show a slight difference of density for the same system (see Figure 3.1). The higher value of density (~0.01 g/cm$^3$) was obtained using the integration time step of 0.2 fs.

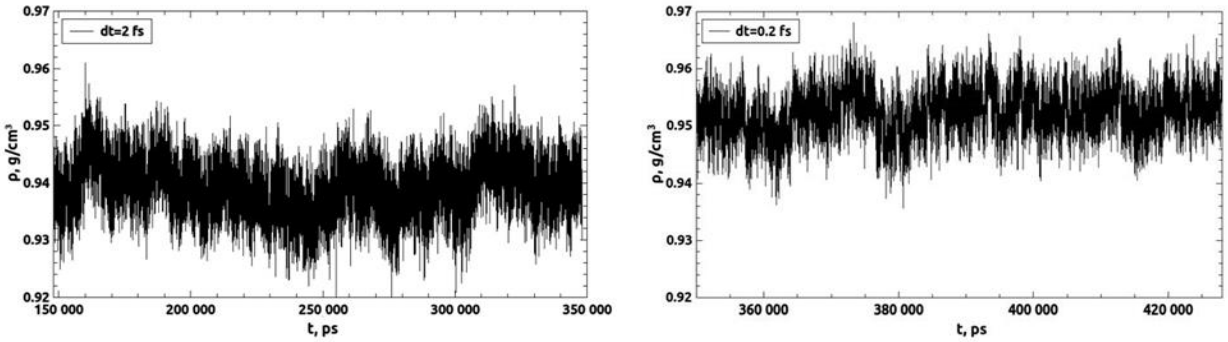


**Figure 3.1** Density of ionic liquid consist of 125 [DMim][Cl] ionic pairs calculated from MD simulations using different integration time steps.

Generally, the liquid structure is described by the site-site radial distribution functions (RDFs). Information from NMR and IR experiments indicate that for imidazolium ILs the most noticeable interactions are those between the acidic hydrogen on the imidazolium ring (H25 in Figure 2.1) and anions. Therefore, to determine the structural properties of the pure [DMim][Cl] ionic liquid, we have calculated the radial distribution functions (RDFs) for this system using different integration time steps at 350K, the results are shown in Figure 3.2. For pure [DMim][Cl], the H25 hydrogen atom of the imidazolium ring is selected to represent the cation, while Cl atom represents the anion, as shown in Figure 2.1. The results revealed that radial distribution functions are almost identical using different integration time steps. On the other hand, the higher probability of finding Cl anion around H25 is observed using shorter integration time step. In both cases, the RDFs have a very sharp first peak centered at around 2.27 Å and the second peak around 6 Å.

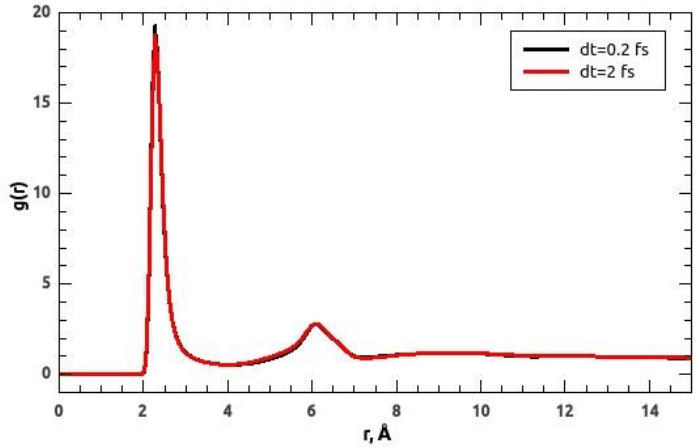


**Figure 3.2** Radial distribution functions of (H25-Cl) in the pure [DMim][Cl] ionic liquid using different integration time steps.

In addition, to understand the influence of different integration time steps on the dynamical property of pure ionic liquid, the mean square displacement (MSD) functions for the $Cl^-$ and the hydrogen atom of the 2nd position of pure [DMim][Cl] ionic liquid have been computed. The typical MSD functions are shown in Figure 3.3 and 3.4 for [DMim][Cl] determined at temperature of 350 K. The results showed that the MSD functions are growing up faster using integration time step of 0.2 fs than with integration time step of 2 fs. The results revealed that the values of the density and parameter of structure practically remain the same using different integration time steps. However, the results of MSDs showed clearly dependence on integration time steps. Unfortunately the MD simulations using shorter integration time step and without SHAKE require much more computational time for the same system so for this reason we decided to use integration time step of 2 fs and SHAKE algorithm for further MD simulations.

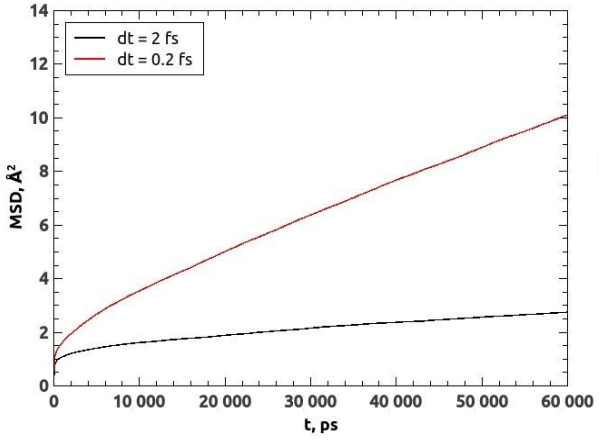


**Figure 3.3** MSDs of Cl anions of pure [DMim][Cl] ionic liquid using different integration time step.

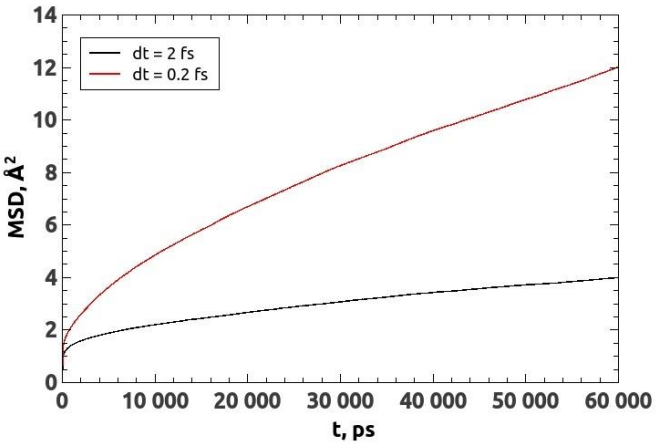


**Figure 3.4** MSDs of 2nd position hydrogen atoms of pure [DMim][Cl] ionic liquid using different integration time step.

### 3.2 The estimation of the cutoff radius

It is known that the structural and dynamical properties of the RTILs could be sensitive to representable of non-bonded interactions. One of the non-bonded interactions is the Van der Waals. Therefore, it is important to select appropriate distance to include a non-bonded interaction in the MD simulations which are always truncated at the cutoff distance, specified by $r_c$. Consequently, to estimate influence of the radius of non-bonded interaction for structural and dynamical properties of pure [DMim][Cl] ionic liquid, we performed MD simulation using different cutoff radii of non-bonded interactions. First of all, the density of pure ionic liquid using different cutoff values for non-bonded interactions were examined and compared. Figure 3.5 shows the comparison of density between different cutoff values (9 Å, 12 Å and 14 Å respectively) which were calculated during 200 ns (cutoff=9 Å) and 150 ns (cutoff=12 Å and 14 Å) isothermal-isobaric MD simulations of [DMim][Cl] at 350 K. It should be noted, that MD simulation was performed using SHAKE algorithm and integration time step was 2 fs for three different cases. The values of density were obtained around 0.94 g/cm$^3$ using different cutoff radii of non-bonded interactions for all cases. These results revealed that different cutoff radius of non-bonded interactions have no significant influence for the density of system.

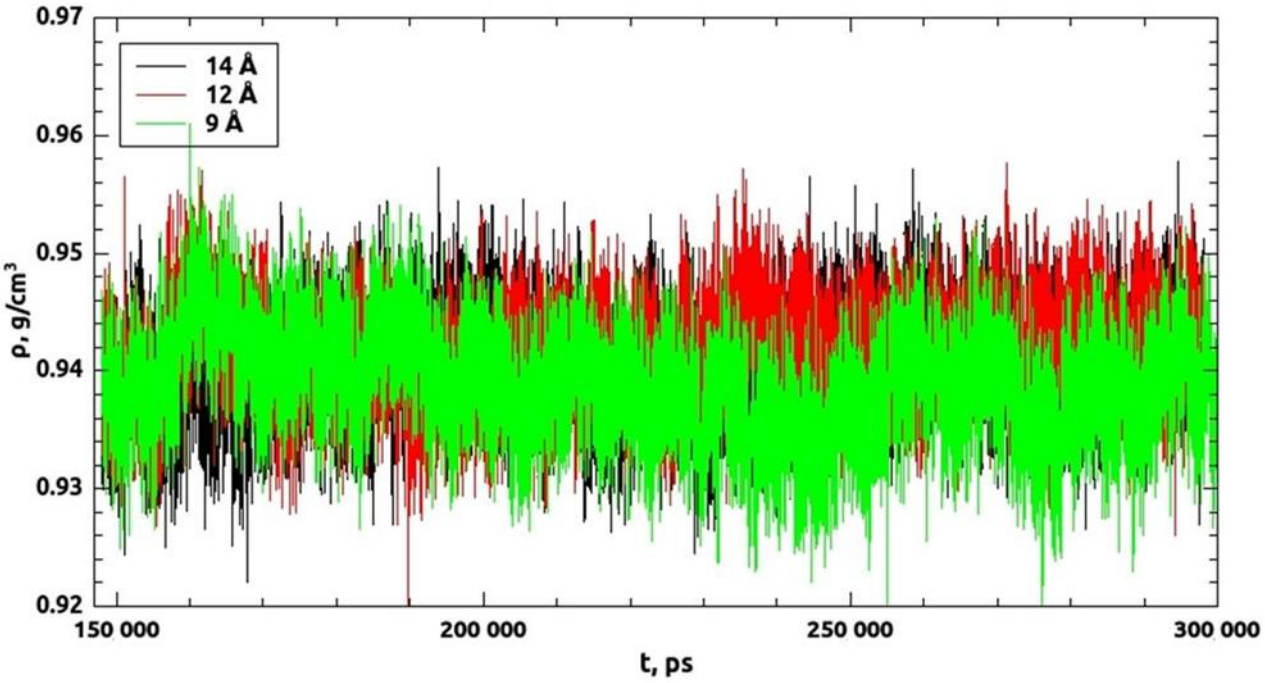


**Figure 3.5** Density of [DMim][Cl] ionic liquid calculated from MD simulations at different cutoff radius of non-bonded interactions.

Also, the RDFs were calculated and compared for the pure [DMim][Cl] ionic liquid using different cutoff radii of non-bonded interactions at 350 K and the results are shown in Figure

3.6. For pure IL system, the H25 hydrogen atom of the imidazolium ring is selected to represent the cation, as shown in Figure 2.1. The results revealed that the radial distribution functions are almost identical using different cutoff radii of non-bonded interactions. On the other hand, the highest probability of finding Cl anion around H25 is observed using cutoff value of 12 Å, while the lowest probability is observed using cutoff value of 14 Å. In all cases, the RDFs have a very sharp first peak centered at around 2.27 Å and the second peak around 6.2 Å. These results also revealed that the different cutoff radii of non-bonded interactions have no significant influence for the structural properties of system.

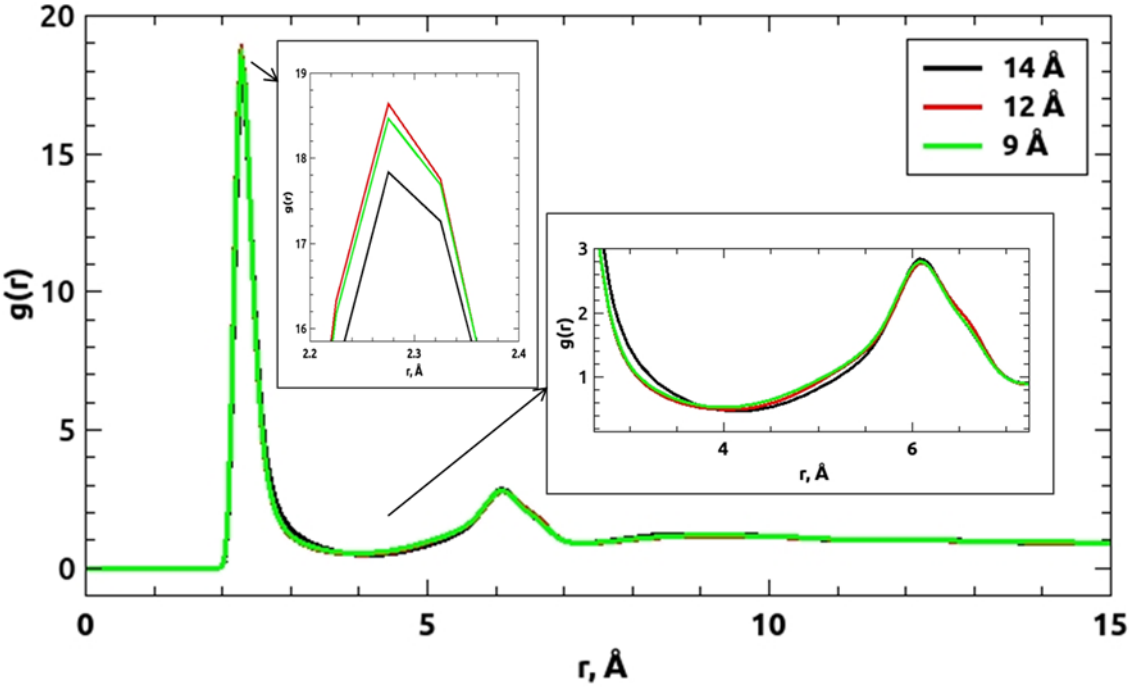


**Figure 3.6** Radial distribution functions (H25-Cl) in the pure [DMim][Cl] ionic liquid at different cutoff radius of non-bonded interactions.

Accordingly, we estimated the influence of different cutoff radii of non-bonded interactions for the dynamical properties of pure ionic liquid. The mean square displacement functions of anions and hydrogen atoms of 2$^{nd}$ position of the pure [DMim][Cl] ionic liquid have been determined. The MSD functions are shown in Figure 3.7 and 3.8 for [DMim][Cl] determined at temperature of 350 K. The results showed that the MSDs are growing up faster using the cutoff value 9 Å with respect to others cutoff values for this system.

The results revealed that the density and structure of this pure ionic liquid are not sensitive to distance of non-bonded interactions included in MD simulation. On the other hand the results of MSD functions showed slight dependence on cutoff value of non-bonded interaction.

According to all of the results, we decided to select shorter integration time step (2 fs)

with SHAKE algorithm and to use cutoff value (9 Å) for further our MD simulations in this work. Because of these selected parameters showed a good agreement with accuracy, computational time and cost.

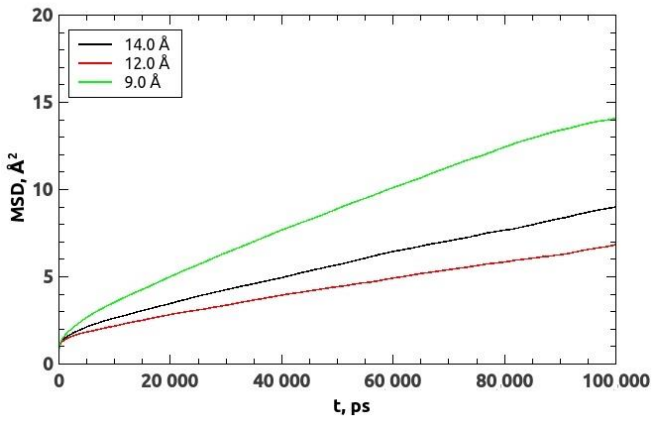


**Figure 3.7** MSDs of Cl anions of pure [DMim][Cl] ionic liquid at different radius of non-bonded interactions.

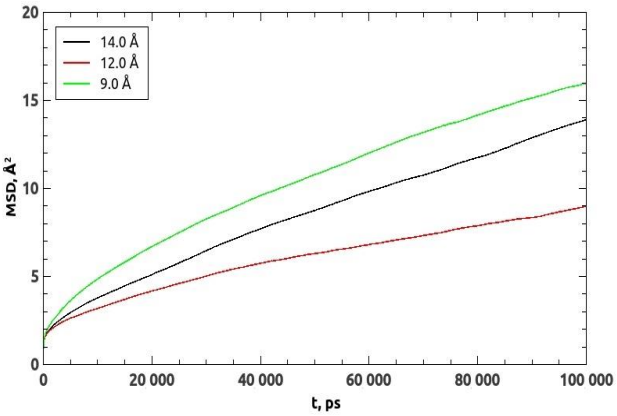


**Figure 3.8** MSDs of 2nd position hydrogen atoms of pure [DMim][Cl] ionic liquid at different radius of non-bonded interactions.

### 3.3 Structural and dynamical properties

#### 3.3.1 The structural properties

##### 3.3.1.1 The density

RTILs are very attractive as recyclable solvents for a range of different applications. Therefore, understanding the effect of water content on local ion−ion, ion−water, and water−water interactions at an atomistic scale is necessary to get better understanding of this solvent. It is well known that interactions between different types of ILs and water solvent are important because ILs can absorb a large amount of water from the atmosphere.[32-36] The solvation properties of ILs strongly depend on their miscibility with water and can be tailored in different ways. So, we performed MD simulations to evaluate the effect of water for the thermodynamic, structural, and mobility properties of mixtures of water with imidazolium-based IL. Firstly, the density of pure ionic liquid which consists of 375 [DMim][Cl] ionic pairs and two [DMim][Cl]/water mixtures were examined and compared. Figure 3.9 shows the comparison of density of the simulated systems (respectively, pure and [DMim][Cl]/water mixture with water molar fraction $\chi_{wat}$ =12 % and $\chi_{wat}$ =46 %). The density was calculated during 1 μs isothermal-isobaric MD simulations of [DMim][Cl] at 350 K. MD simulations were performed using SHAKE[66] algorithm and the integration time step was 2 fs. The obtained density values were obtained around 0.943 g/cm$^3$, 0.956 g/cm$^3$ and 0.973 g/cm$^3$, for pure ionic liquid and its mixtures with low concentration of water

($\chi_{wat}$ =12 %) and high concentration of water ($\chi_{wat}$ =46 %), respectively. As it might be expected since water has a higher density then the IL, a high concentration of water molecules increases the value of density of this very viscous [DMim][Cl] ionic liquid. It is extremely interesting that inspection of the evolution of the density value with time reveals that the pure ionic liquid system reaches equilibrium after 300 ns. The results of density revealed that this ionic liquid requires very long trajectories, in the μs time scale, to reach equilibrium at 350 K. This is a particular meaningful results in view of the lenght of simulations of similar system that are usually presented in literature.

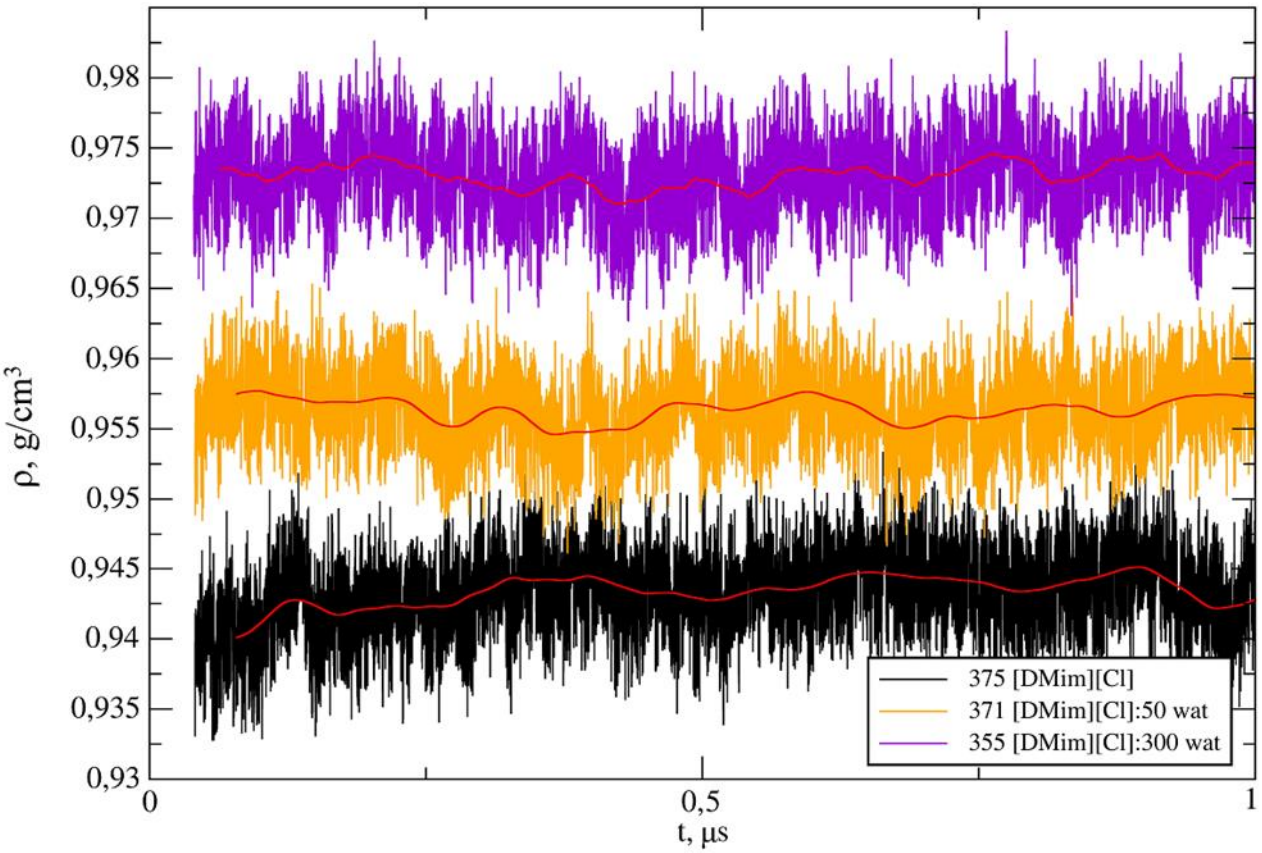


**Figure 3.9** Density of pure [DMim][Cl] ionic liquid and [DMim][Cl]/water mixtures calculated from MD simulations at different concentrations of water

### 3.3.1.2 The radial distribution functions

To determine the effect of water on the structural properties of system, we calculated the radial distribution functions for pure and [DMim][Cl]/water systems with different concentrations of water. Figure 3.10 illustrates RDFs between cation and anion of pure ionic liquid and its mixtures with water ($\chi_{wat}$ =12 % and $\chi_{wat}$ =46 %). The H25 hydrogen atom of the imidazolium ring is selected to represent the cation as shown in Figure 2.1. The results of RDFs revealed that the highest

probability of finding Cl anion around H25 is observed in the pure ionic liquid. In all cases, the RDFs have a very sharp first peak centered at around 2.3 Å and the second peak around 6.15 Å. As the water mole fraction is increased to 46%, the magnitude of the peaks monotonically decreases and the position of first peak maximum is slightly shifted to a larger distance, indicating a weakening in the anion-cation interactions. Similarly, the first minima of RDFs are shifted to larger distances with increasing amount of water in the system. In summary, as indicated by the analyzed RDF the addition of water to [DMim][Cl] do not lead to large structural variation. However the interactions of chlorine with the water molecules lead to a slight decrease in the strength of the interaction with the imidazolium ring.

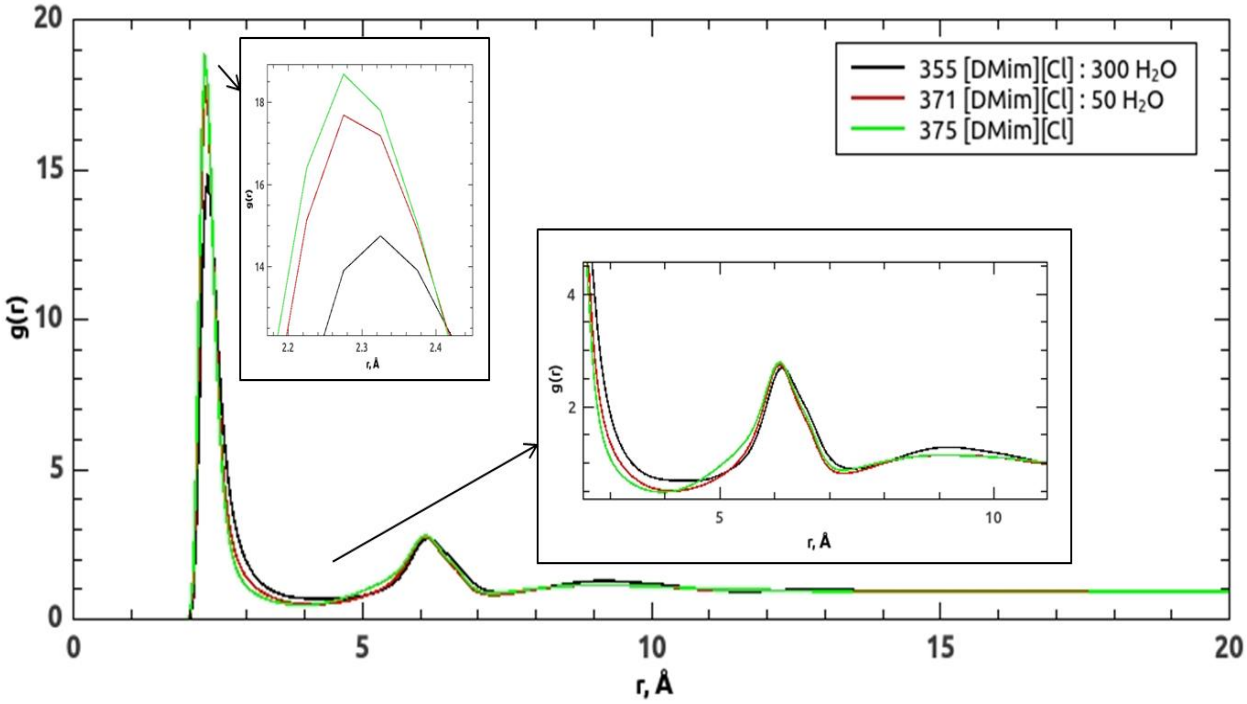


**Figure 3.10** Radial distribution functions (H25-Cl) in the pure [DMim][Cl] ionic liquid and [DMim][Cl]/water mixtures at different concentration of water.

RDF were used also to evaluate the interaction between imidazolium cation and water molecules. Figure 3.11 shows RDFs calculated from MD simulation of [DMim][Cl] with various mole fractions of water ($\chi_{wat}$ =12 % and $\chi_{wat}$ =46 %). The H25 hydrogen atom of the imidazolium ring is selected to represent the cation, while water molecules are represented by their oxygen atoms as shown in Figure 2.1. The highest probability of finding water around H25 is observed in low concentration of water with a first peak centered at around 2.5 Å. Similar behavior is observed in high concentration of water with a peak at 2.4 Å. In this case, other peaks in the RDFs at nearly 5, 6 and 8-9 Å, which are probably due to water molecules bound to the other imidazolium hydrogen

atoms and/or in the solving shell surrounding a coordinated anion or water molecule.

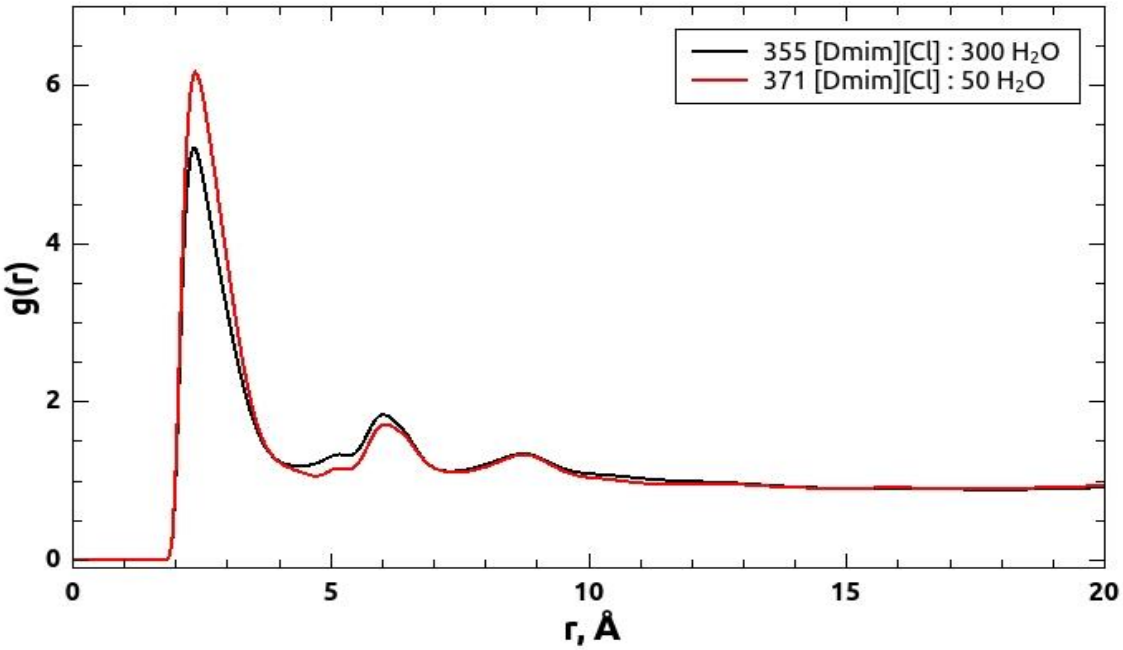


**Figure 3.11** Influence of water concentration on radial distribution functions of [DMim][Cl]/water mixtures: cation-water pairs (H25-O)

### 3.3.2.2 The spatial distribution functions

A qualitative and visually appealing description of the local molecule structure can be obtained by inspection of the spatial distribution function (SDF), using a visualization packages such as gOpenMol[68] or VMD[69]. Figure 3.12 shows SDFs which represent the probability density of finding various atoms around the imidazolium ring. The different colors correspond to SDF of different atoms. The SDFs indicates that there are three major regions where chloride anions are most likely to be found around a cation in liquid [DMim][Cl] and its mixtures with water. Each of these zones is near hydrogens of the imidazolium ring. The same situation is observed for atoms of water (oxygen and hydrogen). Furthermore in Figure 3.12, are represented also the regions with the highest probability of finding the nitrogen atoms N1 and N2, and carbon atoms C1 and C14 of the surrounding organic cations.

The SDFs provide better visualization of probabilities of observing atoms around the imidazolium ring of cation. In our case, the SDFs showed that the structure changes increasing the water content in the system. In addition, increasing water molar fraction the number of SDF peaks increases, being the largest at the highest water concentration. In summary, the SDFs revealed a higher structural organization around cation at increasing concentration of water in the system. Additional SDFs are represented in appendix 1.

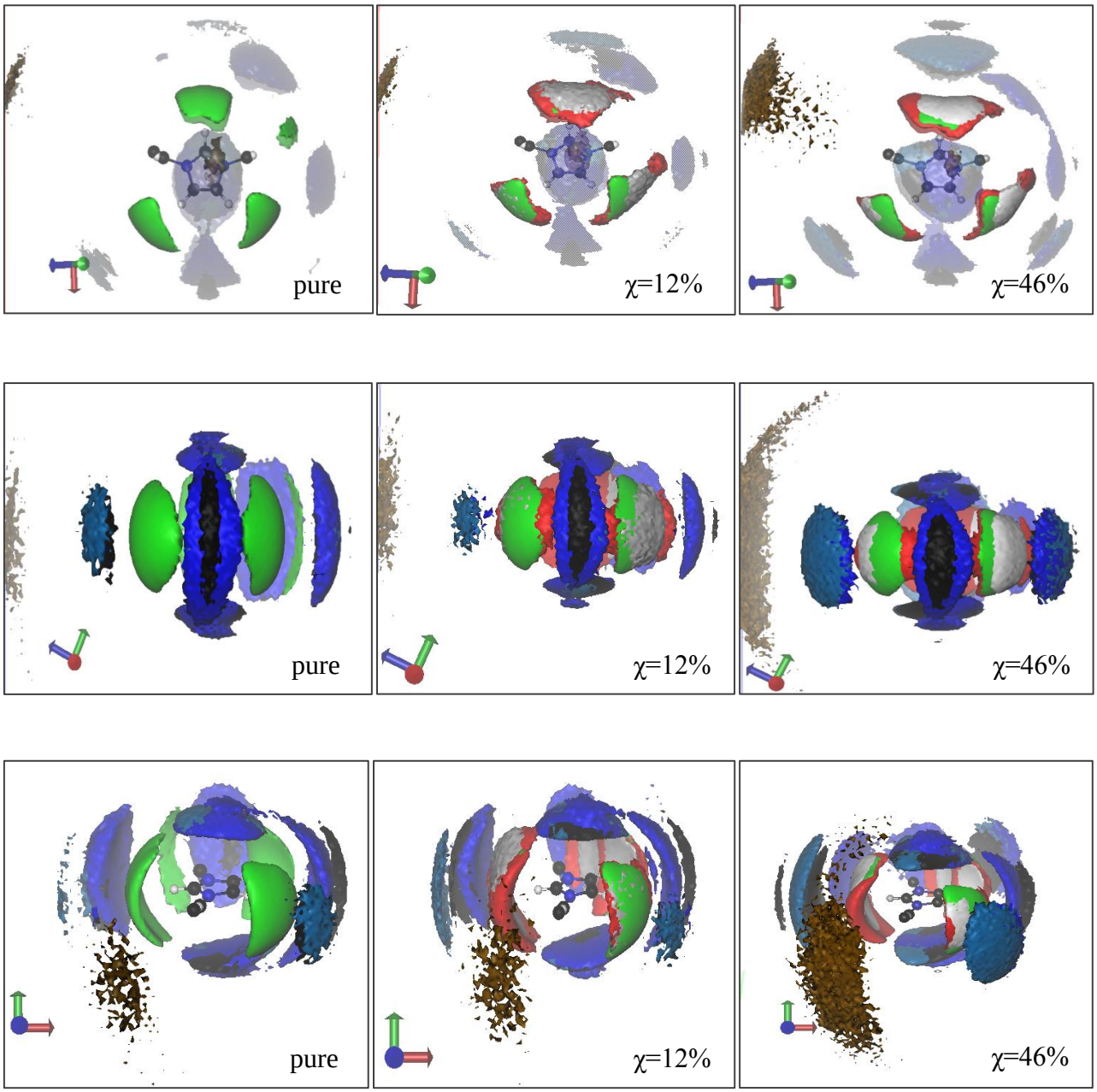


**Figure 3.12** Three-dimensional probability distributions of atoms around cation in pure [DMim][Cl] and its mixtures with water. The isodensity countours correspond to 2.5, 4, 14 and 8 density for C14 atom of cation, C1, N1 and N2 atoms of cation, anion and water, respectively. Colors of atoms are illustrated in Figure 3.13.

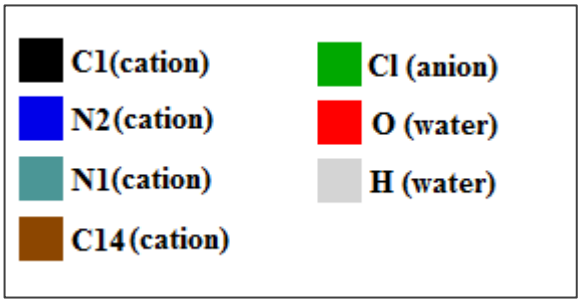


**Figure 3.13** Colors of atoms for SDFs, labeled according to Figure 2.1.

### 3.3.2 The diffusion coefficient

To understand the influence of water content on the dynamical properties of IL/water mixtures, the diffusion coefficients of cations and anions of the [DMim][Cl] and two [DMim][Cl]/water systems have been determined. The diffusion coefficients for all of the systems are determined from the Einstein relation as discussed in section 1.1.7. The mean square displacements (MSDs) of the center-of-mass of the cations and anions of [DMim][Cl] ionic liquid are shown in Figure 3.14, 3.16, 3.18 and 3.20 All MSDs were calculated by using 1 μs ([DMim][Cl]) and 1 μs ([DMim][Cl]/water) MD trajectories with time increments of 100 ps in each case. It is well-known that ILs show very slow dynamics, with diffusion coefficients on the order of $10^{-11}$ $m^2/s$.[55] Therefore it is important to know how long the simulation needs to be continued to compute the MSD and which regime should be used to fit the diffusion coefficient. Cadena et al. have argued[56] that diffusion coefficients determined using MSDs calculated from too short time usually led to an overestimation of the correct values. We have also calculated diffusion coefficients for water molecules moving among the slower particles of the ionic liquid. In Figures 3.15, 3.17, 3.19 and 3.21 are represented the root mean square displacements of the center-of-mass of the water molecule of [DMim][Cl]/water system at 12% and 46% water molar fraction, respectively, where all MSDs were calculated by using and 1 μs MD trajectories with time increments of 100 ps in both cases.

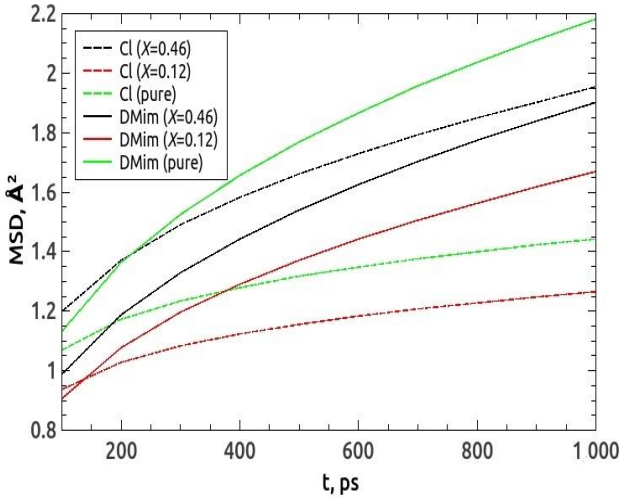


**Figure 3.14** MSDs of cations and anions in [DMim][Cl] at different concentration of water calculated up to 1 ns from a 1 μs MD trajectories.

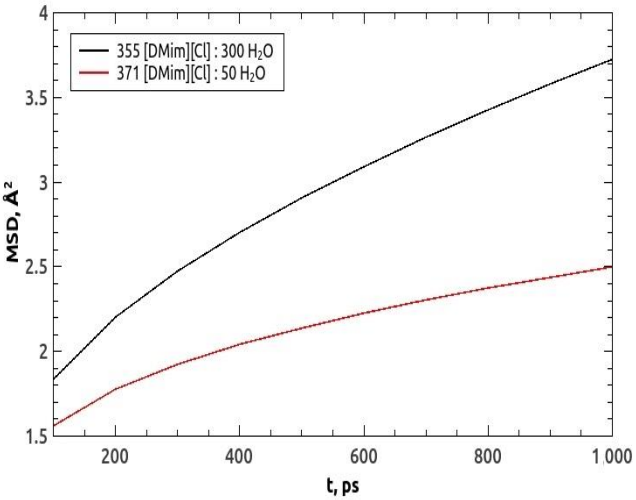


**Figure 3.15** MSDs of water in [DMim][Cl]/water mixtures at different concentration of water calculated up to 1 ns from 1 μs MD trajectories.

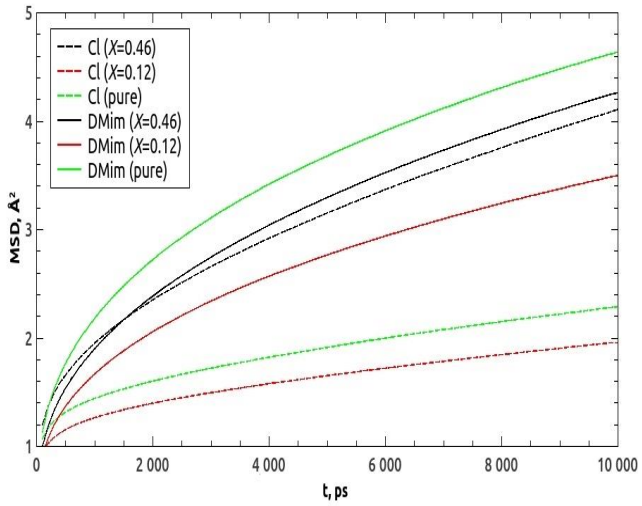


**Figure 3.16** MSDs of cations and anions in [DMim][Cl] at different concentration of water calculated up to 10 ns from 1 μs MD trajectories.

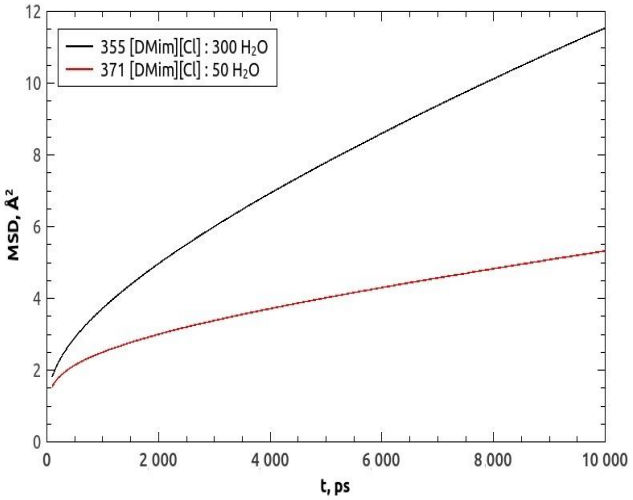


**Figure 3.17** MSDs of water in [DMim][Cl]/water mixture at different concentration of water calculated up to 10 ns from 1 μs MD trajectories.

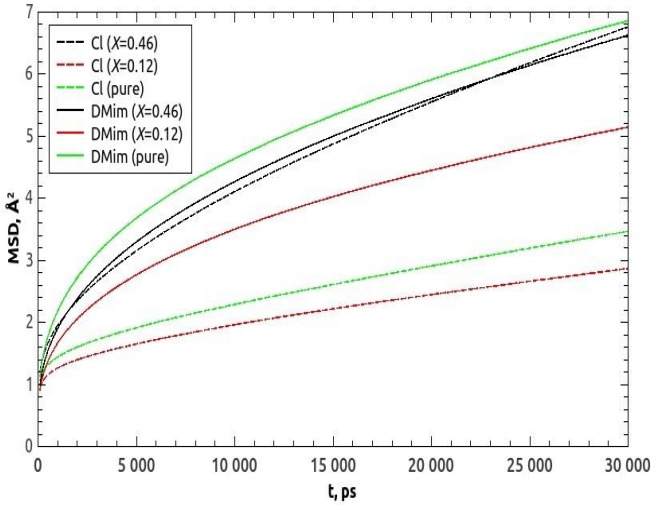


**Figure 3.18** MSDs of cations and anions in [DMim][Cl] at different concentration of calculated up to 30 ns from 1 μs MD trajectories.

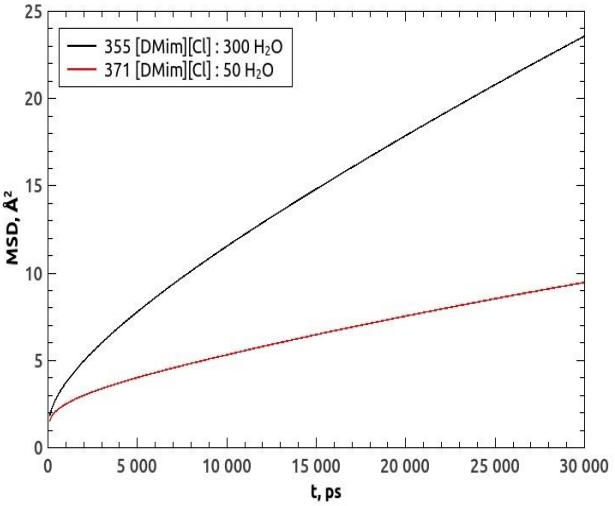


**Figure 3.19** MSDs of water in [DMim][Cl]/water mixture at different concentration of water calculated up to 30 ns from 1 μs MD trajectories.

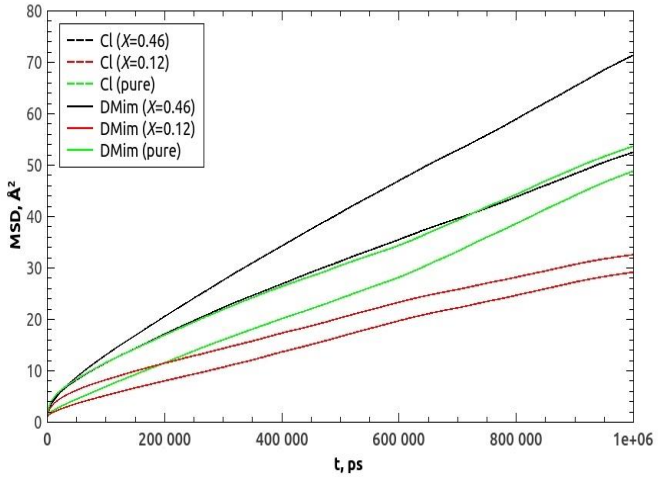


**Figure 3.20** MSDs of cations and anions in [DMim][Cl] at different concentration of water calculated up to 1 μs from 1 μs MD trajectories.

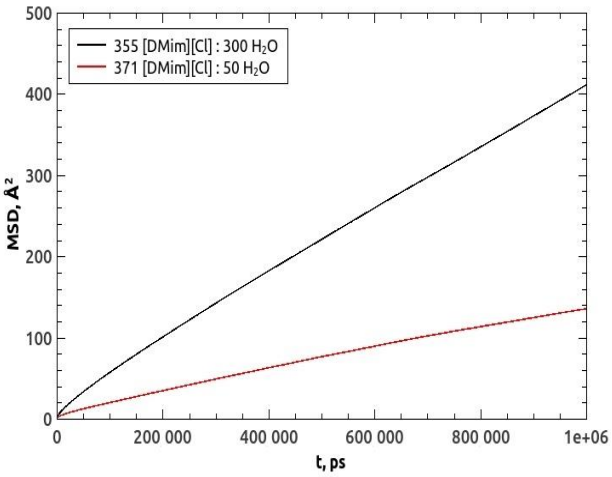


**Figure 3.21** MSDs of water in [DMim][Cl]/water mixture at different concentration of water calculated up to 1 μs from 1 μs MD trajectories.

The diffusion coefficients of the center-of-mass of cations, anions and water molecules as a function of water molar fraction extracted from MSDs functions are shown in Figure 3.22. The results show that the diffusion coefficients are very similar for cations and anions particularly in high concentration of water. Also the same results indicate that the diffusion coefficients of ions slightly decreased in low concentration of water ($\chi_{wat}$=0.12) and noticeably increased in high concentration of water ($\chi_{wat}$=0.46). Unusual trends in the variation of the correlation time characterizing the motion of imidazolium IL with long hydrocarbon chain, has also been observed by Sturlaugson et al.[70] for the [DMim][$BF_4$]/water system when varying water content. Unusual trends were observed only for long alkyl-chain. As expected, water molecules can be displaced more readily than the IL. The diffusion coefficient of water molecules considerably increased (almost three times) in high concentration of water.

As already pointed out above, RTILs show very slow dynamics, with diffusion coefficient (D) on the order of $10^{-11}$ $m^2/s$ at 298 K, to be compared with D ~ $10^{-9}$–$10^{-10}$ $m^2/s$ for simple liquids. This difference is mainly due to the higher viscosity of RTILs.[71] Thus, the much lower D values we obtained for the pure [DMim][Cl] ionic liquid in the present work (see Table 3.1). For clarity, the results of this work were compared with some available references and experimental data which are summarized in Table 3.1. It should be noted that the diffusion coefficients reported here for ILs are derived from non-polarizable the force fields.

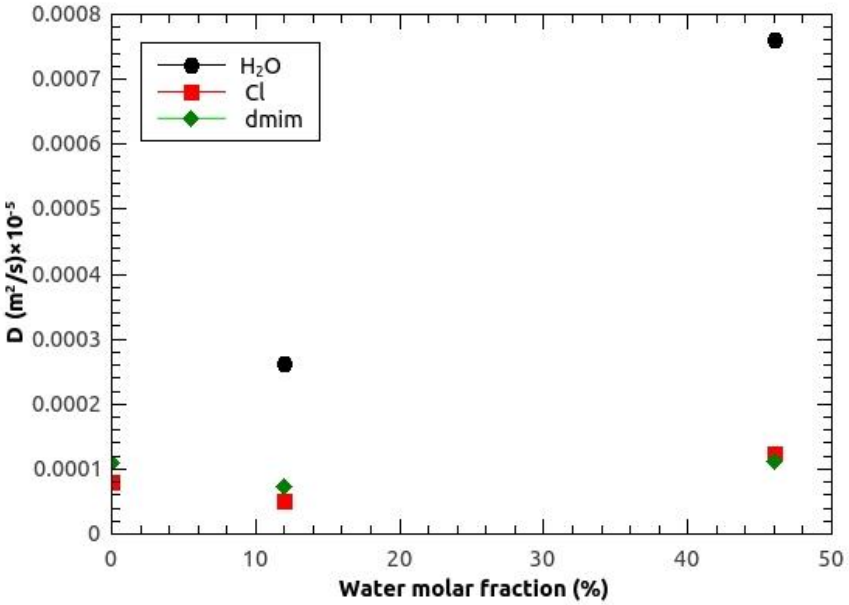


**Figure 3.22** The diffusion coefficients of the center-of-mass of cation, anion and water as a function of water molar fraction calculated from MD simulations.

The results revealed that the diffusion coefficients of the ions in pure IL calculated from our simulation are very similar to experimental data and to other related ILs when, the diffusion coefficients are extracted from short time intervals of MSDs, typically from 500 ps to 1 ns and 10 ns. In order to estimate the impact of the time interval considered for the diffusion constant calculation, we obtained the diffusion using three largely different time intervals, as indicated in Table 3.1. When the time interval of MSD function is rather large (~400 ns), the diffusion coefficients of the ions in pure IL are on the order $10^{-14}m^2/s$, which are 1 or 2 orders of magnitude smaller than that experimental data or others indicated cases. From the comparison of the diffusion constant obtained using different time ranges, it is clear that it highly affect the obtained value. Therefore the mismatches of our results with previously reported computational results could be explained by time interval of MSD which are used to fit the diffusion coefficient rather then on the difference in the parameters of force field.

The diffusion coefficients of the cation and anion in IL/water are very similar to those calculated in the pure ionic liquid. The values of the diffusion coefficients of cations decreased from $0.109 \times 10^{-12}$ $m^2/s$ in zero concentration of water to $0.073 \times 10^{-12} m^2/s$ in low concentration of water and increased to $0.112\times 10^{-12}$ $m^2/s$ in high concentration of water (see Table 3.1 and 3.2). Nevertheless the results reveal that the diffusion coefficients of ions still remain low even in high concentration of water. As it might be expected, the diffusion coefficient of water molecules considerably increased in high concentration of water (see Table 3.2). Notwithstanding, it is found

that the diffusion coefficients of water are three orders of magnitude smaller than the experimental value for water in the ILs at room temperature.[76]

**Table 3.1** The diffusion coefficients of the ILs cations and anions simulated in this work and in the recent literature.

| RTIL (pure) | T, K | D ($10^{-12}$ $m^2$ $s^{-1}$) | time interval the diffusion was extracted from MSD function |
|---|---|---|---|
| **[DMim]$^+$** [Cl]$^-$ | 350 | 4.59[a] | 0.5-1 ns |
| [DMim]$^+$ **[Cl]$^-$** | 350 | 3.23[a] | 0.5-1 ns |
| **[DMim]$^+$** [Cl]$^-$ | 350 | 1.57[a] | 0.5-10 ns |
| [DMim]$^+$ **[Cl]$^-$** | 350 | 0.90[a] | 0.5-10 ns |
| **[DMim]$^+$** [Cl]$^-$ | 350 | 0.43[a] | 20-30 ns |
| [DMim]$^+$ **[Cl]$^-$** | 350 | 0.22[a] | 20-30 ns |
| **[DMim]$^+$** [Cl]$^-$ | 350 | 0.11[a] | 0.6-1μs |
| [DMim]$^+$ **[Cl]$^-$** | 350 | 0.08[a] | 0.6-1μs |
| **[BMim]$^+$** [Cl]$^-$ | 350 | 1.69[b] | 30 ns |
| [BMim]$^+$ **[Cl]$^-$** | 350 | 4.66[b] | 30 ns |
| **[MMim]$^+$** [Cl]$^-$ | 423 | 27[c] | 150 ps |
| [MMim]$^+$ **[Cl]$^-$** | 423 | 18.5[c] | 150 ps |
| **[MMim]$^+$** [Cl]$^-$ | 423 | 48[d] | 10-50 ps |
| [MMim]$^+$ **[Cl]$^-$** | 423 | 41[d] | 10-50 ps |
| **[OMim]$^+$** [Cl]$^-$ | 343 | 1.29[g] | 10-50 ps |
| [OMim]$^+$ **[Cl]$^-$** | 343 | 1.82[g] | 10-50 ps |
| **[DMim]$^+$** [Cl]$^-$ | 318 | 1.7[e] | - |
| **[DMim]$^+$** [Cl]$^-$ | 313 | 0.34[f] | - |

The diffusion coefficients are for the ion indicated in bold. [a]Our work. [b]Niazi et al.[72] [c]Kowsari et al.[72] [d]Liu et al.[66] [g]Liu et al.[74] [e,f]experimental data.[75]

**Table 3.2** The diffusion coefficients of [DMim][Cl]/water mixture of ions and water simulated in this work. Diffusion coefficients are for the ion and water indicated in bold.

| System | T, K | water (mol %) | D ($10^{-12}$ $m^2$ $s^{-1}$) | time interval the diffusion was extracted from MSD function |
|---|---|---|---|---|
| **[DMim]**$^+$ [Cl]$^-$/water | 350 | 0.12 | 3.53[a] | 0.5-1 ns |
| [DMim]$^+$ **[Cl]**$^-$/water | 350 | 0.12 | 2.83[a] | 0.5-1 ns |
| [DMim]$^+$ [Cl]$^-$/**water** | 350 | 0.12 | 5.41[a] | 0.5-1 ns |
| | | | | |
| **[DMim]**$^+$ [Cl]$^-$/water | 350 | 0.12 | 1.19[a] | 0.5-10 ns |
| [DMim]$^+$ **[Cl]**$^-$/water | 350 | 0.12 | 0.25[a] | 0.5-10 ns |
| [DMim]$^+$ [Cl]$^-$/**water** | 350 | 0.12 | 1.76[a] | 0.5-10 ns |
| | | | | |
| **[DMim]**$^+$ [Cl]$^-$/water | 350 | 0.12 | 0.32[a] | 20-30 ns |
| [DMim]$^+$ **[Cl]**$^-$/water | 350 | 0.12 | 0.18[a] | 20-30 ns |
| [DMim]$^+$ [Cl]$^-$/**water** | 350 | 0.12 | 0.57[a] | 20-30 ns |
| | | | | |
| **[DMim]**$^+$ [Cl]$^-$/water | 350 | 0.12 | 0.073[a] | 0.6-1μs |
| [DMim]$^+$ **[Cl]**$^-$/water | 350 | 0.12 | 0.05[a] | 0.6-1μs |
| [DMim]$^+$ [Cl]$^-$/**water** | 350 | 0.12 | 0.263[a] | 0.6-1μs |
| | | | | |
| **[DMim]**$^+$ [Cl]$^-$/water | 350 | 0.46 | 3.96[a] | 0.5-1 ns |
| [DMim]$^+$ **[Cl]**$^-$/water | 350 | 0.46 | 4.21[a] | 0.5-1 ns |
| [DMim]$^+$ [Cl]$^-$/**water** | 350 | 0.46 | 7.67[a] | 0.5-1 ns |
| | | | | |
| **[DMim]**$^+$ [Cl]$^-$/water | 350 | 0.46 | 1.39[a] | 0.5-10 ns |
| [DMim]$^+$ **[Cl]**$^-$/water | 350 | 0.46 | 1.37[a] | 0.5-10 ns |
| [DMim]$^+$ [Cl]$^-$/**water** | 350 | 0.46 | 3.11[a] | 0.5-10 ns |
| | | | | |
| **[DMim]**$^+$ [Cl]$^-$/water | 350 | 0.46 | 0.41[a] | 20-30 ns |
| [DMim]$^+$ **[Cl]**$^-$/water | 350 | 0.46 | 0.42[a] | 20-30 ns |
| [DMim]$^+$ [Cl]$^-$/**water** | 350 | 0.46 | 1.39[a] | 20-30 ns |
| | | | | |
| **[DMim]**$^+$ [Cl]$^-$/water | 350 | 0.46 | 0.112[a] | 0.6-1μs |
| [DMim]$^+$ **[Cl]**$^-$/water | 350 | 0.46 | 0.123[a] | 0.6-1μs |
| [DMim]$^+$ [Cl]$^-$/**water** | 350 | 0.46 | 0.76[a] | 0.6-1μs |

The part of the results of the diffusion coefficients revealed that the dynamics of the pure ionic liquid is rather similar to experimental data. It should be noted, that mentioned results were calculated from relatively short the time interval of MSDs. However, the other results revealed that the dynamics of pure ionic liquid are much slower than in the experimental data when the time interval of MSDs is relatively large. To find out whether this discrepancy could be attributed to

some small amount of water in the experimental sample, we performed calculations of the diffusion coefficients for system with various concentration of water. The results revealed that the dynamics of system is slow even in presence of water. Eventually, all of the results of diffusion coefficients of [DMim][Cl]/water systems revealed that this very viscous RTIL requires proper and precise description of the dynamics. The simulated systems are visualized and their snapshots at different times are represented in appendix 2.

# Conclusions

- The results of MD simulations revealed that the integration time step affects the density and the diffusion of the pure system. Indeed, with an integration time step of 0.2 fs the density is larger than using a 2 fs time step. The integration time step also affects the dynamics of the system, with shorter time step having faster dynamics of the pure system.
- The results revealed that the cutoff radius do not affect the density and the structural properties of the pure system. However, it affects the dynamics, as evaluated by the RMSDs of ions, in not easily predictable way, with the intermediate cutoff value leading to the slowest diffusion constant, and with the lower value leading to the fastest motion.
- On the basis of these results a integration time step of 2 fs and a cutoff of 9 Å were used in the following simulations of the pure ionic liquid and two mixture with water ($\chi_{wat}$=0.12 and $\chi_{wat}$=0.12) and MD simulations in the microsecond time range were produced for all of the systems. A first interesting results is that, as judged from the density of the system, quite long MD simulation time are required at 350 K to reach equilibrium for the pure ionic liquid system; indeed, the density equilibrium value is reached around 300 ns.
- Analysis of the radial and spatial distribution functions for the pure ionic liquid system reveals that the addition of water to [DMim][Cl] leads to a variation in the structural organization. In details, the spatial distribution functions reveal that at higher water content there is a higher degree of order among the organic cations. This indicates that addition of water induces structuring of the system.
- The results of the present work indicates that the value of the diffusion constant varies up to 2 orders of magnitude depending on the time interval used for its calculation. Interestingly, when the diffusion constant is calculated using a short time interval the results obtained are in line with those reported previously in the literature dealing with the simulation of similar systems; If the calculation of the diffusion constant is performed over large time interval (several hundreds of ns), much smaller diffusion constant are obtained, and the agreement with the experimental data is unfortunately worsened.

# References


[1] Welton, T. Chem. Rev. **1999**, *99*, 2071.

[2] Blanchard, L. A.; Hancu, D.; Beckman, E. J.; Bremecke, j. F. Nature **1999**, *399*, 28.

[3] Tzschucke, C. C.; Markert, C.; Bannwarth, W; Roller, S.; Hebel, A.; Haag, R. Angew. Chem,. Int. Ed **2002**, *41*, 3964.

[4] Welton, T.; Wasserscheid, P. *Ionic Liquids and Synthesis*; Wiley-VCH, Weinheim, **2002**.

[5] Welton, T. *Coord. Chem. Rev.* **2004**, *248*, 2459.

[6] Wilkes, J. S. *J. Mol. Catal. A* **2004**, *214*, 11.

[7] Ohno, H. *Electrochemical Aspects of Ionic Liquids*; John Wiley & Sons, **2005**.

[8] Bates, E. D.; Mayton, R.; Ntai, I.; James, H.; Davis, J. *J. Am. Chem. Soc.* **2002**, *124*, 926.

[9] Zhao, H. *Phys. Chem. Liq.* **2003**, *41*, 545.

[10] Hardacre, C.; Holbrey, J. D.; McMath, S. E. J.; Bowron, D. T.; Soper, A. K.; *J. Chem. Phys.* **2003**, *118*, 273.

[11] Deetlefs, M.; Hardacre, C.; Nieuwenhuyzen, M.; Padua, A. A. H.; Sheppard, O.; Soper, A. K. J. *Phys. Chem. B* **2006**, *110*, 12055.

[12] Carper, W.; Wahlbeck, P. G.; Dolle, A. *J. Phys. Chem. A* **2004**, *108*, 868.

[13] Tokuda, H.; Hayamizu, K.; Ishii, K.; Susan, M. A. B. H.; Watanabe, M. *J. Phys. Chem. B* **2004**, *108*, 16593.

[14] Cadena, C.; Zhao, Q.; Snurr, R. Q.; Maginn, E . J. *J. Phys. Chem. B* **2006**, *110*, 2821.

[15] Weingartner, H. *Current Opinion in Colloid and Interface Science* **2013**, *18*, 183.

[16] Koddermann, T,; Wetrz, C.; Heintz, A.; Ludwig, R. *Angew. Chem.* **2006**, *118*, 3780.

[17] Fazio, B.; Triolo, A.; Marco, G. D. *J. Raman. Spectrosc.* **2008**, *39*, 233.

[18] Lopes, J. N. C.; Padua, A. H.; *J. Phys. Chem. B* **2006**, *110*, 3330.

[19] Bagno, A.; D`Amico, F.; Saielli, G. *J. Phys. Chem. B* **2004**, *17*, 131.

[20] Liu, Z,; Huang, S.; Wang, W. *J. Phys. Chem. B* **2004**, *108*, 12978.

[21] Micaelo, N. M,; Baptista, A. M.; Soares, C. M. *J. Phys. Chem. B* **2006**, *110*, 14444.

[22] Dommert, F.; Wendler, K.; Berger, R.; Site, L. D.; Holm, C. *ChemPhysChem* **2012**, *13*, 1625.

[23] Hunt, P. A. *Molecular simulation* **2006,** *32*, 1.

[24] Maginn, E. J. *J. Phys.: Condens. Matter* **2009**, *21*.

[25] Talaty, E. R.; Raja, S.; Storhaug, V. J.; Dolle, A.; Carper, W. R. *J. Phys. Chem. B* **2004**, *108*, 13177.

[26] Gutowski, K. E.; Holbrey, J. D.; Rogers, R. D.; Dixon, D. A. *J. Phys. Chem. B* **2005**, *109*, 23196.

[27] Hunt, P. A.; Gould, I. R. *J. Phys. Chem. A* **2006**, *110*, 2269.

[28] Dong, K.; Zhang, S.; Wang, D.; Yao, X. *J. Phys. Chem. A* **2006**, *110*, 9775.

[29] Koddermann, T.; Wertz, C.; Heintz, A.; Ludwig, R. *ChemPhysChem* **2006**, *7*, 1944.

[30] Seki, S.; Mita, Y.; Tokuda, H.; Ohno, Y.; Kobayashi, Y.; Usami, A.; Watabane, M.; Terada, N.; Miyashiro, H. *Electrochem. Solid-State Lett.* **2007**, *10*, 237.

[31] Seki, S.; Mita, Y.; Tokuda, H.; Ohno, Y.; Kobayashi, Y.; Usami, A.; Watabane, M.; Terada, N.; *J. Phys. Chem. B,* **2006**, *110*, 10228.

[32] Wasserscheid, P., Welton, T., Eds. Ionic Liquids in Synthesis; Wiley-VCH: Weinheim, Germany, **2002**.

[33] Kazarian, S. G.; Briscoe, B. J.; Welton, T.; *Chem. Commun*. **2000**, 2047.

[34] Aki, S. N. V. K.; Brennecke, J.; Samanta, A.; *Chem. Commun*. **2001**, 413.

[35] Tran, C. D.; De Paoli, L.; Silvia, H.; Oliveira, D.; *Appl. Spectrosc*. **2003**, *57*, 152.

[36] Cammarata, L.; Kazarian, S. G.; Salter, P. A.; Welton, T.; *Phys. Chem. Chem. Phys.* **2001**, *3*, 5192.

[37] Seddon, K. R.; Stark, A.; Torres, M. J.; *Pure Appl. Chem.* **2000**, *72*, 2275.

[38] Cammarata, L.; Kazarin, S. G.; Salter, P. A.; Welton, T.; *Physical Chemistry Chemical Physics* **2001**, *3,* 5192.

[39] Hanke, C. G.; Lynden-Bell, R. M.; *The Journal of Physical Chemistry. B* **2003**, *107*, 10873.

[40] Liu, H.; Sale, K. L.; Holmes, B. M.; Simmons, B. A.; Singh, S.; *J. Phys. Chem. B* **2010**, *114*, 4293.

[41] Shen, T.; Langan, P.; French, A.; Johnson, S.; Gnanakaran, G. P. ; *J. Am. Chem. Soc*. **2009**, *131*, 14786.

[42] del Popolo, M. G.; Voth, G. A.; *J. Phys. Chem. B* **2004**, *108*, 1744.

[43] Kowsari, M. H.; Alavi, S.; Ashrafizaadeh, M.; Najafi, B.; *J. Chem. Phys.* **2008**, *129*, 224508.

[44] Raabe, G.; Koehler, J.; *J. Chem. Phys.* **2008**, 129.

[45] Kahlen, J.; Masuch, K.; Leonhard, K.; *Green Chem.* **2010**, *12*, 2172.

[46] Kirschner, K. N.; Woods, R. J.; *Proc. Natl. Acad. Sci. U.S.A.* **2001**, *98*, 10541.

[47] Hanke, C.; Lynden-Bell, R.; *J. Phys. Chem. B* **2003**, *107*, 1087.

[48] Jiang, W.; Wang, Y.; Voth, G. A.; *J. Phys. Chem. B* **2007**, *111*, 4812.

[49] Feng, S.; Voth, G. A.; *Fluid Phase Equilib*. **2010**, *294*, 148.

[50] Hall, C. A.; Le, K. A.; Rudaz, C.; Radhi, A.; Lovell, C. S.; Damion, R. A.; Budtova, T.; Ries, M. E.; *J. Phys. Chem. B* **2012**, *116*, 12810.

[51] Meller, J. *Nature Publishing Group,* **2001**, *12*, 1.

[52] Frenkel, D.; Smit, B. *Understanding Molecular Simulation;* Academic Press: New York, **1996**.

[53] Allen, M. P.; Tildesley, D. J. *Computer simulation of liquids*, Clarendon Press, Oxford, **1987**.

[54] Hünenberger, P. H. *Adv. Poly. Sci.*, **2005**, *173*, 105.

[55] Gonzalez, M. A. *Collection SFN* **2011**, *12*, 169.

[56] Gavezzotti, A; *Molecular Aggregation: Structure analysis and molecular simulation of crystals and liquids*, Oxford University Press, **2007.**

[57] Mackerell, A. D. et al.*; J. Chem. Phys.*, **1998**, *102*, 3586.

[58] Cornell W. D. et. al.; *J. Am. Chem. Soc.*, **1995**, *117*, 5179.

[59] Oostenbrink, C.; Villa, A.; Mark, A. E.; van Gunsteren W. F.; *J. Comput. Chem.*, **2004**, *25*, 1656.

[60] Jorgesen, W. L.; Maxwell, D. S.; Tirado-Rives, J.; *J. Am. Chem. Soc.*, **1996**, *118*, 11225.

[61] Sun, H.; *J. Phys. Chem.*, **1998**, *102*, 7338.

[62] Mocci, F.; Laaksonen A.; Wang, Y.; Saba, G.; Lai, A.; Marincola, F. C.; *The structure of ionic liquids*, Springer International Publishing Switzerland, **2014.**

[63] Liu, Z.; Chen, T.; Bell, A.; Smit, B.; *J. Phys. Chem. B* **2010,** *114*, 4572.

[64] Case, D. A.; Babin, V.; Berryman, J. T.; Betz, R. M.; Cai, Q.; Cerutti, D.S.; Cheatham, T. E.; III, Darden, T. A.; Duke, R. E.; Gohlke, H.; Goetz, A. W.; Gusarov, S.; Homeyer, N.; Janowski, P.; Kaus, J.; Kolossváry, I.; Kovalenko, A.; Lee, T. S.; LeGrand, S.; Luchko, T.; Luo, R.; Madej, B.; Merz, K. M.; Paesani, F.; Roe, D. R.; Roitberg, A.; Sagui, C.; Salomon-Ferrer, R.; Seabra, G.; (**2014**), AMBER 14, University of California, San Francisco.

[65] Martínez, L.; Andrade, R.; Birgin, E. G.; Martínez, J. M.; Packmol: A package for building initial configurations for molecular dynamics simulations. *Journal of Computational Chemistry*, 30(13):2157-2164, **2009**.

[66] Liu, Z.; Huang, S. and Wang, W.; *J. Phys. Chem. B* **2004,** *108*, 12978.

[67] Frenkel, D.; Smit, B. *Understanding Molecular Simulation;* Academic Press: New York, **1996**.

[68] L. Laaksonen, A graphics program for the analysis and display of molecular dynamics trajectories. *J. Mol. Graphics*, **1992**, *10*, 33.

[69] Humphrey, W., Dalke, A. and Schulten, K., "VMD - Visual Molecular Dynamics", *J. Molec. Graphics*, **1996**, *14*, 33.

[70] Sturlaugson, A. L.; Fruchey, K. S.; Fayer, M. D.; *J. Phys. Chem. B* **2012**, *116*, 1777.

[71] Weingärtner, H.; *Angew. Chem. Int. Ed.* **2008**, *47*, 654.

[72] Niazi, A. A.; Rabideau, B. D.; Ismail, A. E.; *J. Phys. Chem. B* **2013**, *117*, 1378.

[73] Kowsari, M. H.; Alavi, S.; Ashrafizaadeh, M.; Najafi, B.*; J. Chem. Phys.* **2008**, *129*, 224508.

[74] Liu, Z.; Chen, T.; Bell, A.; Smit, B.; *J. Phys. Chem. B* **2010,** *114*, 4572.

[75] Klimavicius, V.; Bacevicius. V.; Gdaniec, Z.; Balevicius, V.; *Journal of Molecular Liquids*, **2015**, 210, 223.

[76] Saihara,K; Yoskimura, Y; Ohta, S; Shimizu, A; *Scientific report*, **2015**, *5*, 10619.

# Summary

Dovilė Lengvinaitė

## MOLECULAR DYNAMICS SIMULATIONS OF 1-DECYL-3-METHYL-IMIDAZOLIUM CHLORIDE IONIC LIQUID AND ITS MIXTURES WITH WATER

In the last several years, RTILs have become an interesting class of solvents for different chemical applications and required a better understanding of their physical and chemical properties. The family of ILs based on imidazolium cations has been intensively investigated due to their desirable physical and chemical properties. A number of experimental and theoretical studies of imidazolium-based ILs have focused on understanding the interactions between different types of ILs and water solvent. Understanding such interaction is of great importance because ILs can absorb a large amount of water from the atmosphere. This is relevant due to the fact that even low levels of water in ILs can dramatically change their physical and chemical properties such as viscosity, density conductivity and solvating ability.

The aim of this work is to study the structural and dynamical properties of the ionic liquid 1-decyl-3-methyl-imidazolium chloride ([DMim][Cl]) and investigate how they are affected by the presence of water molecules.

The main results: A first interesting results is that, as judged from the density of the system, quite long MD simulation time are required at 350 K to reach equilibrium for the pure ionic liquid system; Analysis of the radial and spatial distribution functions for the pure ionic liquid system reveals that the addition of water to [DMim][Cl] leads to a variation in the structural organization. In details, the spatial distribution functions reveal that at higher water content there is a higher degree of order among the organic cations. This indicates that addition of water induces structuring of the system.

The results of the present work indicates that the value of the diffusion constant varies up to 2 orders of magnitude depending on the time interval used for its calculation. Interestingly, when the diffusion constant is calculated using a short time interval the results obtained are in line with those reported previously in the literature dealing with the simulation of similar systems; If the calculation of the diffusion constant is performed over large time interval (several hundreds of ns), much smaller diffusion constant are obtained, and the agreement with the experimental data is unfortunately worsened.

# Santrauka

Dovilė Lengvinaitė

## JONINIO SKYSČIO 1-DECIL-3-METIL-IMIDAZOLO CHLORIDO IR JO MIŠINIŲ SU VANDENIU MOLEKULINĖS DINAMIKOS SIMULIACIJOS

Pastaruosius keletą metų joniniai skysčiai yra plačiai tyrinėjami dėl jų potencialaus pritaikymo įvairiose srityse. Tai yra vieni įdomiausių tirpiklių, todėl geresnis šių skysčių cheminių ir fizikinių savybių supratimas yra būtinas. Viena iš svarbiausių užduočių yra išsiaiškinti joninių skysčių ir vandens sąveikų savybes. Tokių sąveikų supratimas yra labai svarbus, nes joniniai skysčiai gali absorbuoti didelį kiekį vandens molekulių iš aplinkos. Žinoma, kad net nedidelis kiekis vandens, pastebimai, įtakoja joninių skysčių fizikines ir chemines savybes, tokias kaip tankis, klampumas, laidumas.

Šio darbo tikslas yra ištirti joninio skysčio 1-decil-3-metil-imidazolo chlorido struktūrinius ir dinaminius parametrus bei įvertinti vandens molekulių poveikį šiems parametrams.

MD simuliacijų rezultatai atskleidė, kad sistemos struktūriniai parametrai nepriklauso nuo integravimo žingsnio ir Van der Valso sąveikų radiuso vertės. Tačiau sistemos difuzijos koeficientas yra jautrus minėtų parametrų vertėms.

Sistemų tankio rezultatai atskleidė, kad gryno joninio skysčio sistemai pasiekti pusiausvyrą yra reikalinga gana ilga MD simuliacija esant 350 K temperatūrai. Šios sistemos pusiausvyra yra pasiekiama ~300 ns. RPFs parodė sistemų struktūrinius pakitimus didėjant vandens koncentracijai.

Difuzijos koeficiento rezultatai atskleidė, kad gryno joninio skysčio difuzijos vertės sutampa eilės ribose su eksperimentiniais duomenimis. Didėjant vandens koncentracijai sistemoje, difuzijos koeficientų vertės padidėja iki kelių kartų.

**Appendix 1.**

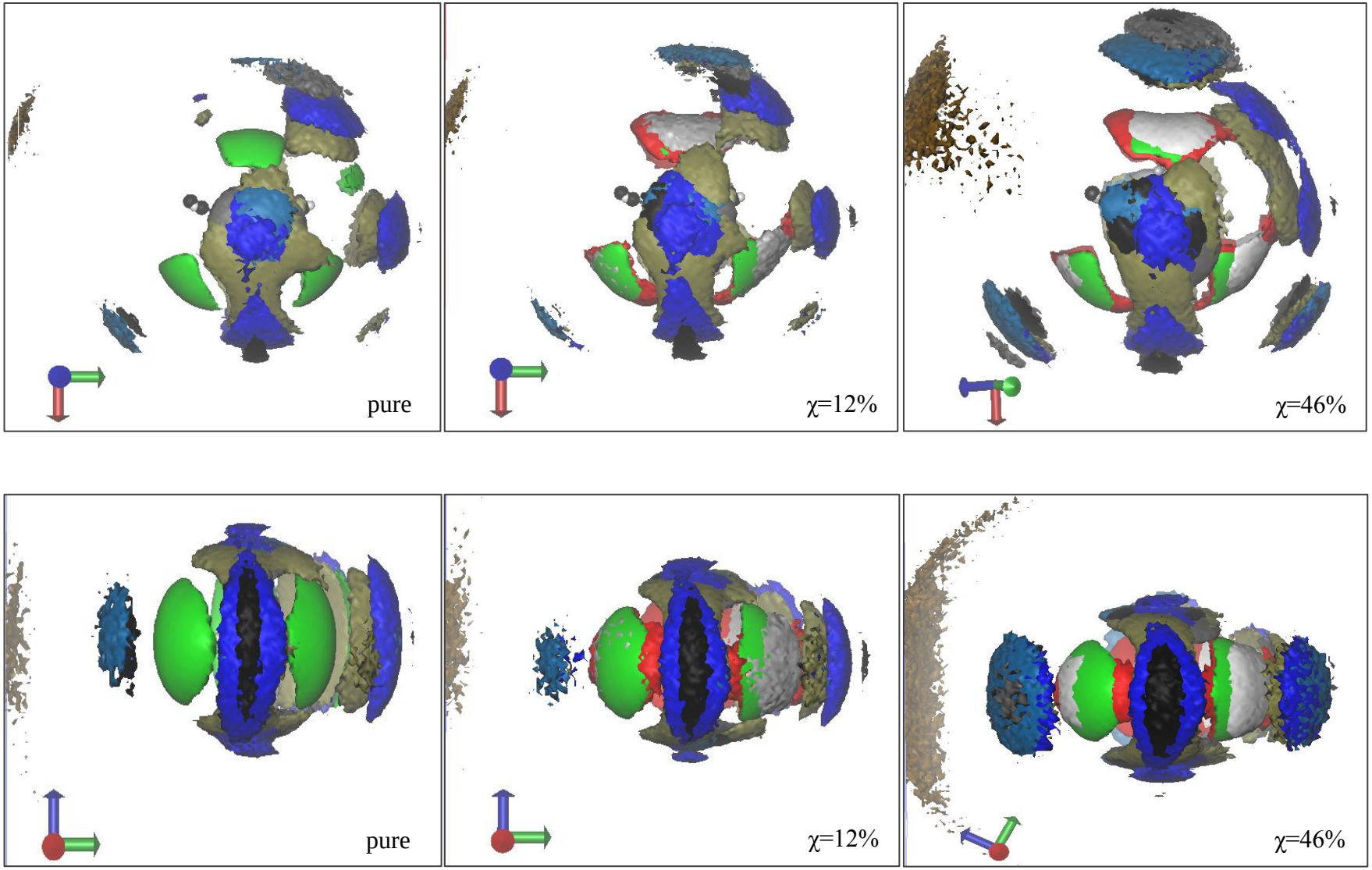

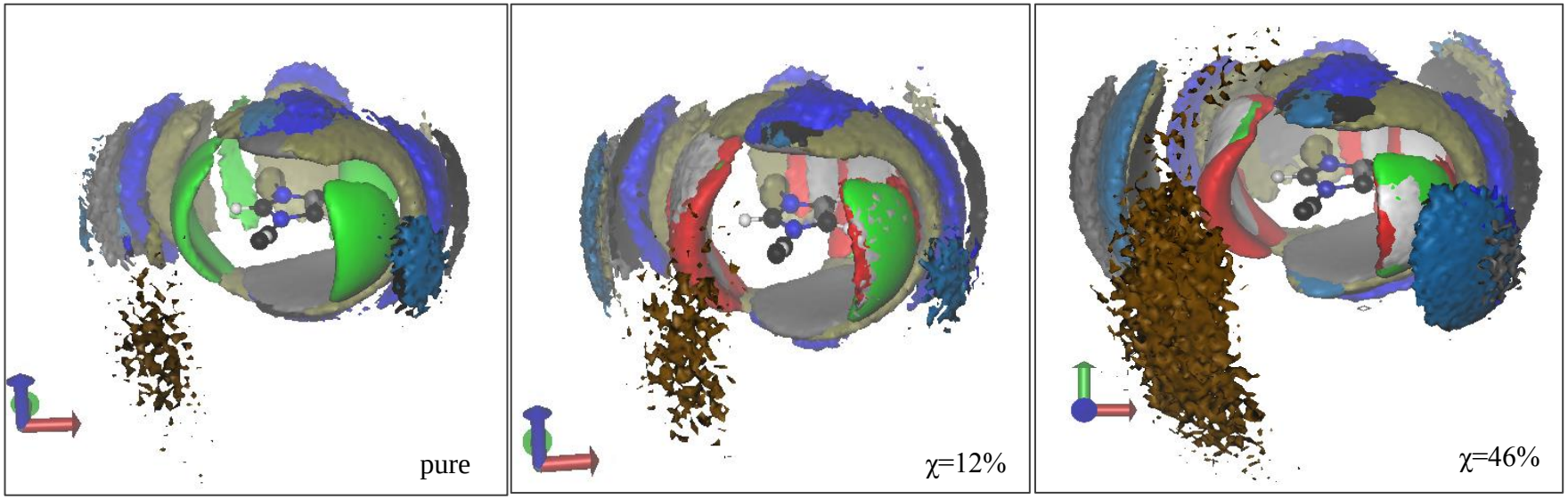


**Figure 1** Three-dimensional probability distributions of atoms around cation in pure [DMim][Cl] ionic liquid and its mixtures with water. The isodensity countours correspond to 2.5 ,4, 14 and 8 density for C14 atom of cation, C1, C2, C5, N1 and N2 atoms of cation, anion and water, respectively. Colors of atoms are illustrated in Figure 1.1.

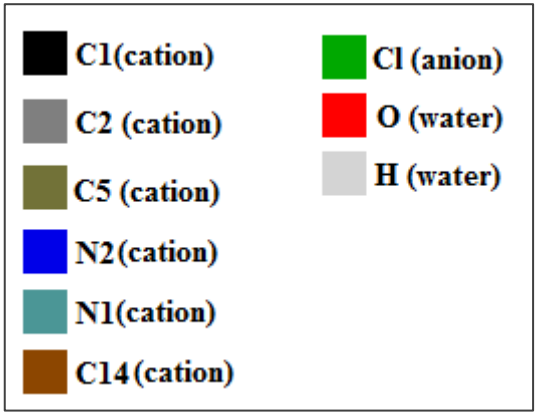


**Figure 1.1** Colors of atoms for SDFs, labeled according to Figure 2.1.

**Appendix 2.**

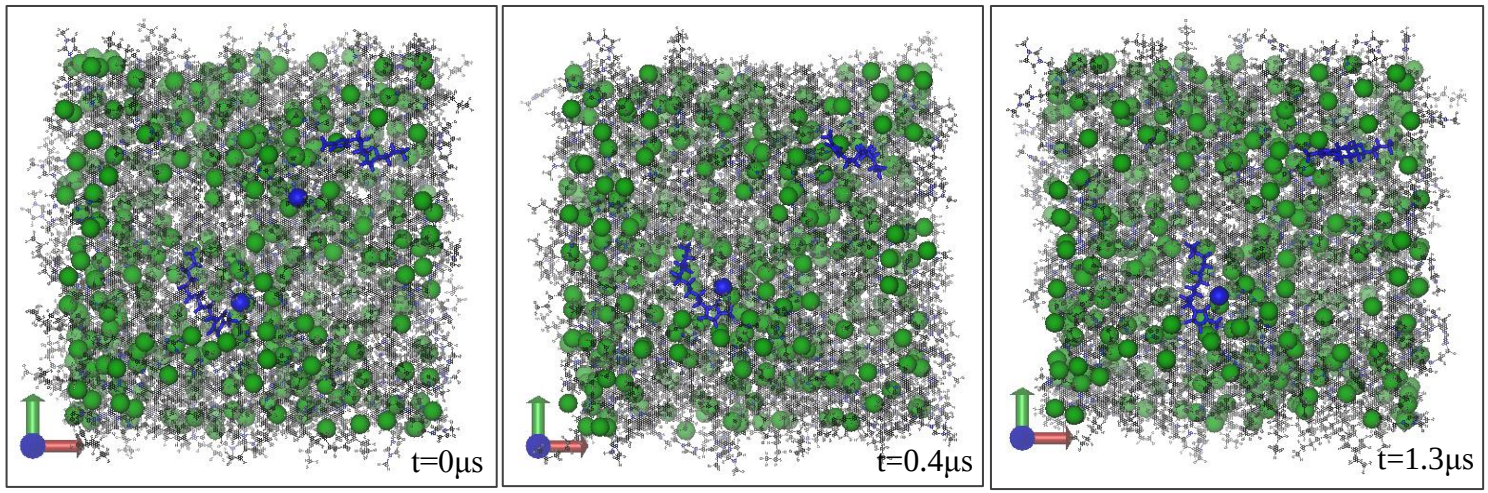


**Figure 1** Snapshots of MD simulation boxes pure [DMim][Cl] IL at different times. The cations are colored grey while anions – green, only two ionic pairs are colored a blue for better visualization of motion of the system.

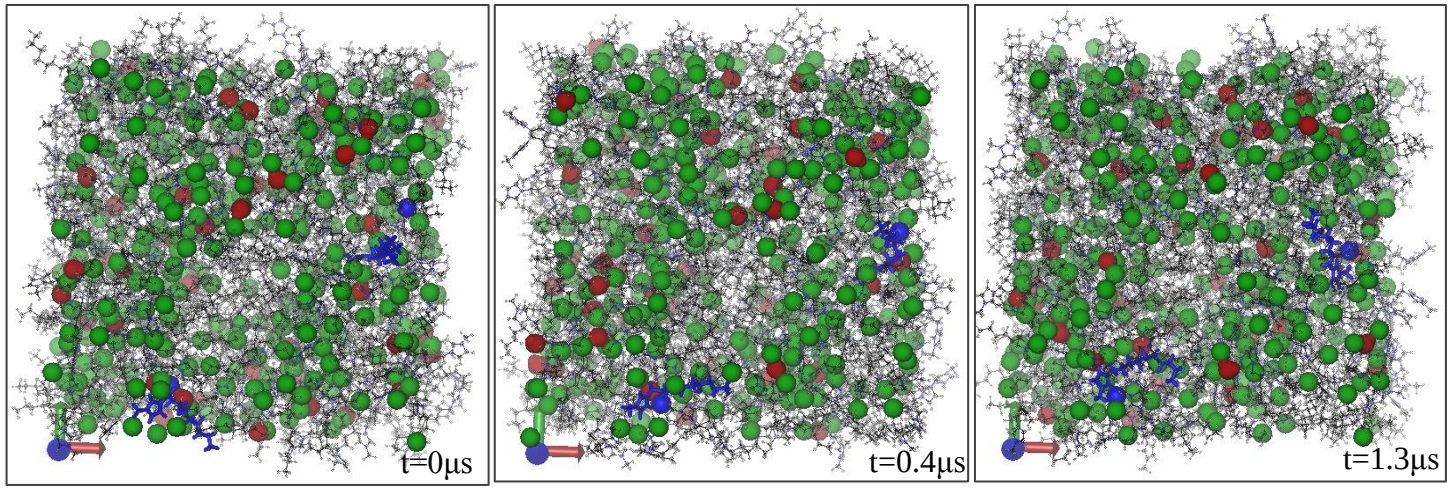


**Figure 2** Snapshots of MD simulation boxes [DMim][Cl]/water mixture (χ=0.12%) at different times. The cations are colored grey while anions – green, and water – red, only two ionic pairs are colored a blue for better visualization of motion of the system.

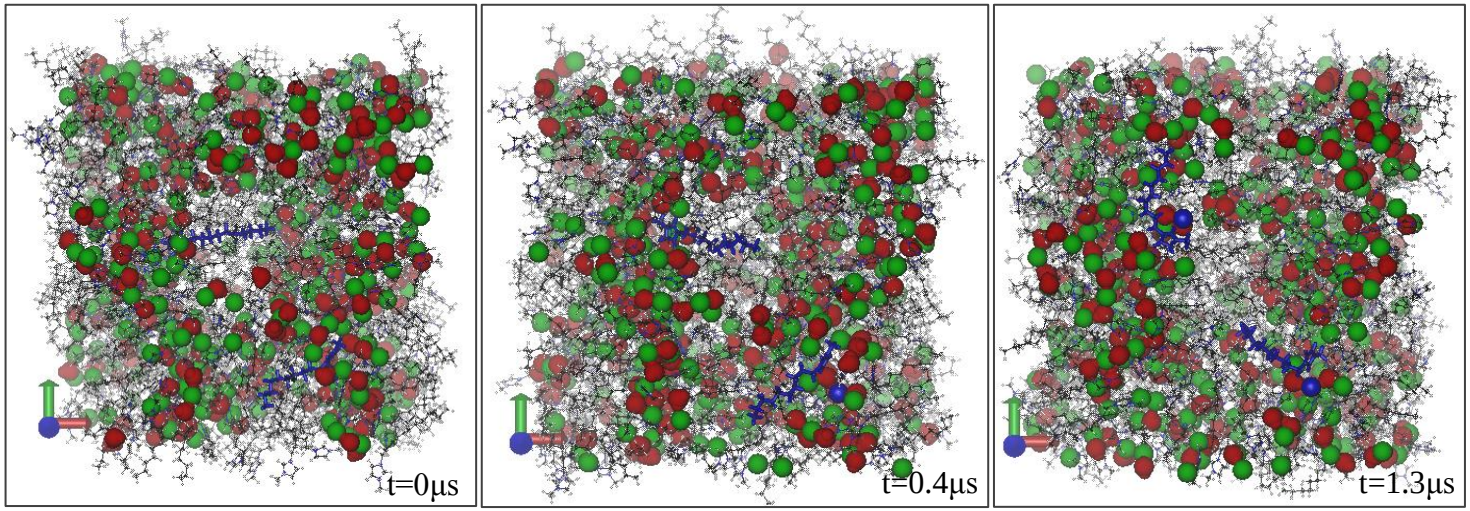


**Figure 3** Snapshots of MD simulation boxes [DMim][Cl]/water mixture ($\chi$=0.46%) at different times. The cations are colored grey while anions – green, and water – red, only two ionic pairs are colored a blue for better visualization of motion of the system.